TURUN YLIOPISTON JULKAISUJA
ANNALES UNIVERSITATIS TURKUENSIS

SARJA - SER. D OSA - TOM. 1074

MEDICA - ODONTOLOGICA

MAGNETIC RESONANCE IMAGING METHODS IN THE FOLLOW-UP OF MULTIPLE SCLEROSIS AND IN FABRY DISEASE

by

Teemu Paavilainen

TURUN YLIOPISTO
UNIVERSITY OF TURKU
Turku 2013

From the Department of Diagnostic Radiology, Institute of Clinical Medicine, Faculty of Medicine and Turku Doctoral Programme of Clinical Sciences, University of Turku, Turku, Finland

Supervised by

Professor Riitta Parkkola, MD, PhD
Department of Radiology
University of Tampere
Tampere, Finland

Docent Laura Airas, MD, PhD
Department of Neurology
University of Turku
Turku, Finland

Docent Timo Kurki, MD, PhD
Department of Radiology
University of Turku
Pulssi Medical Centre
Turku, Finland

Reviewed by

Docent Auli Verkkoniemi-Ahola MD, PhD
Department of Neurology
University of Helsinki
Helsinki, Finland

Docent Tapani Tikkakoski, MD, PhD
Department of Radiology
Keski-Pohjanmaa Central Hospital
Kokkola, Finland

Opponent

Docent Juhana Hakumäki, MD, PhD
Department of Radiology
University of Eastern Finland
Kuopio, Finland

ISBN 978-951-29-5422-3 (PRINT)
ISBN 978-951-29-5423-0 (PDF)
ISSN 0035-9483
Painosalama Oy - Turku, Finland 2013

To Teija, Venla and Anni

ABSTRACT

Teemu Paavilainen
MAGNETIC RESONANCE IMAGING METHODS IN THE FOLLOW-UP OF MULTIPLE SCLEROSIS AND IN FABRY DISEASE
From the Department of Diagnostic Radiology
University of Turku, Turku, Finland
Annales Universitatis Turkuensis SER. D TOM.1074, Painosalama Oy,Turku, Finland 2013
ISBN 978-951-29-5422-3 (PRINT), ISBN 978-951-5423-0 (PDF), ISSN 0035-9483

Multiple sclerosis (MS) is a chronic immune-mediated inflammatory disorder of the central nervous system. MS is the most common disabling central nervous system (CNS) disease of young adults in the Western world. In Finland, the prevalence of MS ranges between 1/1000 and 2/1000 in different areas.

Fabry disease (FD) is a rare hereditary metabolic disease due to mutation in a single gene coding α-galactosidase A (α-gal A) enzyme. It leads to multi-organ pathology, including cerebrovascular disease. Currently there are 44 patients with diagnosed FD in Finland.

Magnetic resonance imaging (MRI) is commonly used in the diagnostics and follow-up of these diseases. The disease activity can be demonstrated by occurrence of new or Gadolinium (Gd)-enhancing lesions in routine studies. Diffusion-weighted imaging (DWI) and diffusion tensor imaging (DTI) are advanced MR sequences which can reveal pathologies in brain regions which appear normal on conventional MR images in several CNS diseases.

The main focus in this study was to reveal whether whole brain apparent diffusion coefficient (ADC) analysis can be used to demonstrate MS disease activity. MS patients were investigated before and after delivery and before and after initiation of disease-modifying treatment (DMT). In FD, DTI was used to reveal possible microstructural alterations at early timepoints when excessive signs of cerebrovascular disease are not yet visible in conventional MR sequences.

Our clinical and MRI findings at 1.5T indicated that post-partum activation of the disease is an early and common phenomenon amongst mothers with MS. MRI seems to be a more sensitive method for assessing MS disease activity than the recording of relapses. However, whole brain ADC histogram analysis is of limited value in the follow-up of inflammatory conditions in a pregnancy-related setting because the pregnancy-related physiological effects on ADC overwhelm the alterations in ADC associated with MS pathology in brain tissue areas which appear normal on conventional MRI sequences.

DTI reveals signs of microstructural damage in brain white matter of FD patients before excessive white matter lesion load can be observed on conventional MR scans. DTI could offer a valuable tool for monitoring the possible effects of enzyme replacement therapy in FD.

Keywords: Multiple sclerosis, pregnancy, Fabry disease, magnetic resonance imaging, diffusion-weighted imaging, diffusion tensor imaging

TIIVISTELMÄ

Teemu Paavilainen
MAGNEETTIKUVAUSMENETELMÄT MS-TAUDIN SEURANNASSA JA FABRYN TAUDISSA
Diagnostisen radiologian klinikka,
Turun Yliopisto, Turku
Annales Universitatis Turkuensis SER. D TOM.1074, Painosalama Oy,Turku, Finland 2013
ISBN 978-951-29-5422-3 (PRINT), ISBN 978-951-29-5423-0 (PDF), ISSN 0035-9483

MS-tauti on yleisin immuunivälitteinen keskushermoston krooninen sairaus. Suomessa taudin esiintyvyys vaihtelee välillä 1-2/1000, ja se on yli kaksi kertaa yleisempi naisilla kuin miehillä. Suurin osa MS-tautitapauksista ilmenee 20-45 ikävuoden välillä.

Fabryn tauti on harvinainen X-kromosomissa periytyvä aineenvaihdunnallinen sairaus, jossa α-galaktosidaasi A-entsyymin puutos johtaa sfingolipidien kertymiseen soluihin, mikä aiheuttaa vakavia komplikaatioita useissa kohde-elimissä.

Magneettikuvausta käytetään yleisesti keskushermoston tautien diagnostiikassa ja seurannassa. MS-taudin aktiivisuus voidaan osoittaa mm. magneettikuvissa näkyvien uusien tai Gadoliniumilla tehostuvien plakkien perusteella. Diffuusio- ja diffuusiotensorikuvaus ovat uudempia magneettikuvauksen menetelmiä, joiden kontrasti perustuu vesimolekyylien liikkeen eroavaisuuksiin toisaalta normaalin harmaan ja valkean aineen välillä ja toisaalta normaalin ja poikkeavan aivokudoksen välillä. Näillä menetelmillä on mahdollista osoittaa poikkeavuuksia, jotka eivät erotu “tavanomaisissa” magneettikuvissa.

Tämän tutkimuksen päätarkoituksena oli selvittää, voidaanko diffuusiokuvausta käyttää raskaana olevien MS-potilaiden tautiaktiivisuuden seurannassa, sekä tutkia millaisia muutoksia tapahtuu MS-potilaiden aivokudoksessa interferonilääkityksen aloittamisen jälkeen. Lisäksi tutkimme, voidaanko diffuusiotensorikuvauksella löytää poikkeavuuksia Fabry-potilaiden aivokudoksesta myös sellaisilla alueilla, jotka näyttävät normaaleille tavanomaisissa magneettikuvissa.

Tutkimuksemme perusteella MS-taudin aktivoituminen muutamien viikkojen kuluttua synnytyksestä on hyvin tavallista, minkä osoittivat sekä 1.5 Teslan magneettikuvauslöydökset että MS-taudin pahenemisvaiheiden moninkertainen lisääntyminen synnytyksen jälkeen. Magneettikuvaus on herkkä menetelmä osoittamaan synnytyksen jälkeinen MS-taudin aktivoituminen. Diffuusiokuvauksen luotettavuutta MS-taudin aktivoitumisessa synnytyksen jälkeen rajoittavat aivoissa tapahtuvat raskauteen liittyvät fysiologiset muutokset.

Diffuusiotensorikuvauksella voidaan nähdä merkkejä Fabryn taudin aiheuttamista valkean aineen ratojen vaurioista laajoilla aluilla jo silloin, kun tavanomaissa magneettikuvissa on vielä niukasti Fabryn taudin aiheuttamia muutoksia.

Avainsanat: MS-tauti, raskaus, Fabryn tauti, magneettikuvaus, diffuusiopainotteinen kuvaus, diffuusiotensorikuvaus

TABLE OF CONTENTS

ABBREVIATIONS AND DEFINITIONS

AD	axial diffusivity
ADC	apparent diffusion coefficient
α-gal A	α-galactosidase A
BA	basilar artery
BBB	blood-brain barrier
BET	Brain Extraction Tool
BVI	brain volume index
CC	corpus callosum
CIS	clinically isolated syndrome
CNS	central nervous system
CSF	cerebrospinal fluid
DMT	disease-modifying treatment
DTI	diffusion tensor imaging
DWI	diffusion-weighted imaging
EBV	Epstein-Barr virus
EDSS	Expanded Disability Status Scale
EPI	echo-planar imaging
ERT	enzyme replacement therapy
FA	fractional anisotropy
FAST	FMRIB´s Automated Segmentation Tool
FD	Fabry disease
FDT	FMRIB´s Diffusion Toolbox
FLAIR	fluid-attenuated inversion recovery
FLIRT	FMRIB´s Linear Image Registration Tool
FMRIB	Functional MR Imaging of the Brain
FNIRT	FMRIB´s Nonlinear Registration Tool
FSL	FMRIB´s Software Library
GA	glatiramer acetate
Gb3	globotriaocylceramide
Gd	gadolinium
IFN-β	interferon-beta

JCV	John Cunningham virus
MD	mean diffusivity
MELAS	mitochondrial encephalomyopahty, lactic acidosis and stroke-like episodes
mFs	modified Fazekas score
MNI 152	Montreal Neurologic Institute 152
MRI	magnetic resonance imaging
MS	multiple sclerosis
MTR	magnetization transfer
NAGM	normal-appearing grey matter
NAWM	normal-appearing white matter
PBVC	percentage brain volume change
PML	progressive multifocal leukoencephalopathy
PPMS	primary progressive multiple sclerosis
PRMS	progressive-relapsing multiple sclerosis
RD	radial diffusivity
RF	radio frequency
RRMS	relapsing-remitting multiple sclerosis
SD	standard deviation
SEM	standard error of mean
SIENA	Structural Image Evaluation using Normalization of Atrophy
SIENAX	adaptation of SIENA for cross-sectional measurement
SPM	Statistical Parametric Mapping
SPMS	secondary progressive multiple sclerosis
TBSS	Tract-Based Spatial Statistics
TE	echo time
TR	repetition time
VBM	voxel-based morphometry
WML	white matter lesion

LIST OF ORIGINAL PUBLICATIONS

This thesis is based on the following original publications, which are referred to in the text by Roman numerals I-IV.

I. Paavilainen T, Kurki T, Parkkola R, Färkkilä M, Salonen O, Dastidar P, Elovaara I, Airas L. Magnetic resonance imaging of the brain used to detect early post-partum activation of multiple sclerosis. Eur J Neurol 2007; 14: 1216-1221.

II. Paavilainen T, Kurki T, Färkkilä M, Salonen O, Parkkola R, Airas L. Lower brain diffusivity in postpartum period compared to late pregnancy: results from a prospective imaging study of multiple sclerosis patients. Neuroradiology 2012; 54: 823-828.

III. Paavilainen T, Kurki T, Korhonen K, Airas L. Apparent Diffusion Coefficient Histograms in the Follow-up of Relapsing-Remitting Multiple Sclerosis. The Neuroradiology Journal 2009; 22: 22-28.

IV. Paavilainen T, Lepomäki V, Saunavaara J, Borra R, Nuutila P, Kantola I, Parkkola R. Diffusion tensor imaging and brain volumetry in Fabry disease patients. Neuroradiology 2013, in press.

1. INTRODUCTION

Multiple sclerosis (MS) is a chronic demyelinating disease of the central nervous system (CNS). It is the most common disabling CNS disease of young adults in the Western world (Compston and Coles 2002). MS is about 2.5 times more common in females than in males and commonly affects women of reproductive age.

MS has been divided into four different subtypes (Lublin and Reingold 1996). Initially, 80% of the MS patients present a relapsing-remitting MS (RRMS), in which relapses with random intervals are followed by remission, i.e. partial or complete recovery (Noseworthy et al. 2000).

The aetiology of MS is unknown and seems to be multifactorial. Genetic factors are involved to some extent (Chao et al. 2011), but there are also several environmental factors that seem to increase the risk of MS including Epstein Barr virus (EBV) infection (Ascherio and Munger 2007), vitamin D deficiency (Munger et al. 2004) and smoking (Hedström et al. 2009).

There are no curative therapies for MS currently available. The purpose of MS therapy is to reduce the frequency of acute relapses, to shorten their duration and to thus to provide relief of symptoms (Cree 2007). The first line treatment of MS includes interferon beta (IFN-β) and glatiramer acetate (GA). Early commencement of treatment has been shown to reduce the occurrence of relapses and development of disability (Clerico et al. 2008; Comi et al. 2001; Jacobs et al. 2000; Kappos et al. 2007).

Pregnancy modulates MS disease activity and is typically a stabilising period in the clinical course of the disease. During the third trimester the relapse rate can be approximately 70% lower relative to the year before pregnancy (Confavreux et al. 1998). In contrast, aggravation of the disease is commonly seen soon after delivery (Vukusic and Confavreux 2006; Vukusic et al. 2004)

Fabry disease (FD) is a rare X-linked metabolic disease first described by Johannes Fabry in Germany (Fabry 1898) and William Anderson in England (Anderson 1898). The incidence of FD has been estimated to be 1 per 111,700 live births (Spada et al. 2006). Currently there are 44 patients (30 females, 14 males) with diagnosed FD in Finland (Kantola et al. 2012).

In FD, sfingolipids accumulate to cells because of α-galactosidase A (α-gal A) enzyme deficiency. As a consequence, a multi-organ pathology occurs, most seriously affecting the kidneys, heart and cerebrovascular system (Clarke 2007; Zarate and Hopkin 2008). As an X-linked disease, FD affects all hemizygous males who exhibit the classic phenotype of FD due to minimal or completely missing α-gal A activity. In male patients, the FD typically reduces lifespan by approximately 15-20 years. Most heterozygous female FD patients are clinically affected but there is more variability in the clinical course of the disease, depending on the level of α-gal A-activity (MacDermot et al. 2001; Whybra et al. 2009)

There is no curative therapy for FD. Enzyme replacement therapy (ERT) has been shown to slow down the development of major organ complications and to improve the quality of life. In Finland, ERT preparations have been in systematic use since 2004 (Kantola et al. 2012).

Magnetic resonance imaging (MRI) is the method of choice for imaging pathological conditions of the CNS. It offers superior contrast compared to computed tomography without the use of ionising radiation. In MS and FD, the most typical imaging findings in conventional MRI scans are variable sized lesions appearing bright on T2-weighted sequences. In FD, the lesions are of ischemic aetiology, whereas in MS, a wide range of histopathological processes, such as demyelination (Estes et al. 1990), inflammation (Nesbit et al. 1991), oedema (Ormerod et al. 1987), and gliosis (Stewart et al. 1986), may result in visible hyperintensities in T2-weighted sequences.

Despite the differences in typical imaging findings between MS and vascular diseases, they cannot always be differentiated on the basis of single MR imaging. In addition to vascular diseases, other demyelinating diseases, neurosarcoid, lyme disease and CNS fungal diseases are also included in the differential diagnosis of MS.

In FD, the shape and distribution of the lesions are nonspecific and have features of both large-vessel (cortical infarcts) and small-vessel (lacunar infarcts and scattered leukoaraiotic lesions) disease. In MS, typical lesion distribution differs from the typical distribution of small-vessel ischemic lesions. Typical MS lesion distribution involves the corpus callosum, juxtacortical (touching cortical grey matter) and temporal white matter, which is atypical for leukoaraiotic lesions. MS lesions typically have an ovoid shape and are perpendicular to the ventricles. In the brain stem, vascular lesions are typically located centrally, whereas MS lesions usually have a peripheric location. MS lesions enhancing with Gadolinium are considered as a sign of recent disease activity.

Diffusion-weighted imaging (DWI) and diffusion tensor imaging (DTI) are MR sequences which can reveal pathologies in brain regions which appear normal on conventional MR images. The contrast of DWI and DTI images is based on differences in the random thermal motion of water in different brain regions, and it provides quantitative information about the tissue structure. In DTI, the most commonly used parameter to quantitate white matter integrity is fractional anisotropy (FA).

There are numerous reports of MRI findings in MS patients. Moreover, DWI and DTI have been used to explore MS, and have revealed pathologies in brain regions that appear normal on conventional MR scans (Gallo et al. 2005; Roosendaal et al. 2009). However, there are no previous longitudinal reports of pregnant MS patients imaged with MRI and DWI. There are also only a few longitudinal studies using DWI in MS patients with DMT (Sämann et al. 2012). In FD, a few studies with DWI and DTI have been performed (Albrecht et al. 2007; Fellgiebel et al. 2006a; Moore et al. 2002). These studies have revealed an increase of mean diffusivity (MD) or apparent diffusion coefficient (ADC) in normal appearing brain tissue, but have not revealed abnormalities on FA.

The aim of the present study was to explore the nature of alterations taking place in the

brain tissue of RRMS patients in relation to pregnancy and delivery, and after initiation of DMT. MR data was correlated with clinical signs of disease activation both before and after delivery and before and after the initiation of treatment. The main focus was, using DWI, to follow possible changes taking place in brain tissue which appeared normal on conventional MR images. Furthermore, we performed a voxelwise DTI study with FD patients to reveal possible microstructural alterations before excessive ischemic lesion load is visible on conventional MR sequences.

2 REVIEW OF THE LITERATURE

2.1. Multiple sclerosis

MS is a chronic immune-mediated inflammatory demyelinating disorder, which can affect any part of the CNS, but most commonly white matter tracts in the cerebral hemispheres, brainstem, cerebellum and spinal cord (Morales et al. 2005). The lifetime risk of MS is about 1 in 400, and it is the most common neurological condition affecting young adults in the Western world. About 80% of patients are diagnosed between the ages of 20 and 45 years (Compston and Coles 2002). Finland is among the high risk regions for MS (Compston 1997; Kurtzke 1977), with prevalences ranging between 100 and 200 per 100,000 population (Sumelahti et al. 2000; 2001).

Clinically isolated syndrome (CIS) is a term used to describe a first clinical episode in which patient has signs and symptoms suggesting inflammatory demyelinating disorder of the CNS (Miller DH et al. 2008). About 85% of patients with MS experience onset of the disease with CIS (Confavreux and Vukusic 2006; Scalfari et al. 2010). MS has been divided into four subtypes (Lublin and Reingold 1996), but the two main subtypes of MS are considered to be relapsing-remitting MS (RRMS) and primary-progressive MS (PPMS), comprising 80% and 20% of MS cases respectively. In RRMS, relapses with random intervals are followed by remission, i.e. partial or complete recovery (Noseworthy et al. 2000), whereas PPMS presents from onset with continuous clinical deterioration without relapse or remission (Compston and Coles 2002). Approximately 65% of patients with RRMS will later transition to secondary progressive MS (SPMS), in which the patient's clinical deterioration is also on-going without interposing remission periods (Compston and Coles 2002). A rare form of MS is progressive-relapsing MS (PRMS), which is characterised by continuing progression with subsequent relapses superimposed onto on-going progression (Lublin and Reingold 1996).

Clinically, the disease severity is estimated using the Expanded Disability Status Scale (EDSS) ranging from 0 to 10, in which EDSS 0.0 means no disability, EDSS 6.0 means that the patient needs intermittent or constant assistance to walk about 100 metres with or without resting, and EDSS 10.0 means death due to MS (Kurtzke 1983). There are a number of other rating scales to assess the morbidity of MS, such as the Multiple Sclerosis Severity Score (Roxburgh et al. 2005), Multiple Sclerosis Functional Composite (Cutter et al. 1999) and Multiple Sclerosis Impact Scale (Hobart et al. 2001). Self-assessment scales of MS disease status include the Patient-Determined Disease Steps (Kister et al. 2013) and Patient-Derived MS severity score (Vollmer et al. 1999).

The aetiology of MS is unknown but is, without a doubt, multifactorial. Genetic factors are involved to some extent, and to date, nearly 100 associated genes have been identified (Chao et al. 2011). Several infectious agents have been suggested as triggers of MS, including for example Epstein Barr virus (EBV), human herpes virus 6, and

Chlamydia pneumoniae. Of these, only EBV has so far been proved to be a consistent and strong risk factor of MS (Ascherio and Munger 2007). Important environmental and lifestyle-associated factors also have an influence on the evolution of MS. The use of a dietary vitamin D supplement has been shown to significantly reduce the risk of MS development (Munger et al. 2004). A decreased relapse rate and appearance of new lesions in MRI in paediatric-onset MS has been also been attributed to the use of vitamin D supplement (Mowry et al. 2010; Mowry et al. 2012). Both active (Hedström et al. 2009; Hernán et al. 2001; Riise et al. 2003) and passive smoking (Hedström et al. 2011b) are risk factors for MS. Furthermore, smoking seems to increase the risk of RRMS transforming into SPMS (Hernán et al. 2005). Shift work at a young age increases the risk of developing MS, which may be associated with a disturbance in melatonin secretion and enhanced proinflammatory responses (Hedström et al. 2011a).

2.1.1. Diagnosis of MS

An MS diagnosis requires evidence of dissemination of the disease process both in time and space. The diagnosis is made clinically with the help of paraclinical tools including MRI, cerebrospinal fluid (CSF) analysis (showing evidence of intrathecal synthesis of oligoclonal bands or IgG), visual, brainstem or somatosensory evoked potentials. The McDonald criteria (McDonald et al. 2001) for MS and subsequent revisions (Polman et al. 2011; Polman et al. 2005) have incorporated MRI and laboratory testing into the diagnostic scheme and have enabled an earlier diagnosis of MS following a single clinical monosymptomatic event. According to the revised McDonald criteria, the diagnosis of MS can be made on the basis of a single MRI exam, if both enhancing and non-enhancing lesions are seen and the clinical criteria are fulfilled (Elovaara et al. 2012).

2.1.1.1. MRI findings in MS

The most characteristic pathological features in MS are plaques i.e. areas of inflammatory demyelination located in the brain and/or spinal cord. They appear typically as variable-sized hyperintense foci on T2-weighted, proton density and FLAIR imaging. Typical MS lesion distribution involves the corpus callosum, juxtacortical (touching cortical grey matter) and temporal white matter, which is atypical for leukoaraiotic lesions. MS lesions also have a typically ovoid shape, and they are often perpendicular to the ventricles. In the brain stem, vascular lesions are typically located centrally, whereas MS lesions usually have peripheric location. A wide range of histopathological processes in MS, such as demyelination (Estes et al. 1990), inflammation (Nesbit et al. 1991), oedema (Ormerod et al. 1987) and gliosis (Stewart et al. 1986) may result in visible hyperintensities in the above-mentioned MR sequences. Hence, it is not possible to determine specific histopathological correlates for any given T2-imaging abnormality in brain MR images of an MS patient. The correlation between T2 lesion load and clinical disability is often poor. This phenomenon is frequently referred to as the clinico-radiological paradox (Barkhof 2002).

Low-signal lesions in T1-weighted images are less prevalent. The prevalence of lesions having as low signal as that of CSF, so-called "black holes", often increases during the transition of the disease into a secondary progressive phase. They may indicate areas of irreversible tissue damage, probably because of axonal loss and gliosis (van Walderveen et al. 1998). The load of T1 "black holes" has a better correlation with clinical disability than T2-lesion load has (Truyen 1996). T1-weighted images obtained after Gd permit the identification of new or acute lesions and reflect damage in the blood-brain barrier (BBB) (Grossman et al. 1986).

MS lesions are not limited to the brain white matter, but cortical and deep grey matter is also frequently affected (Kidd et al. 1999). It has been shown that using 3T MRI with a double inversion recovery sequence improves MS lesion detection compared to 1.5T. The improvement of lesion detection with 3T is more prominent in grey than in white matter (Simon et al. 2010). Using 7T MRI further improves grey matter, but not white matter, MS lesion detection (de Graaf et al. 2013).

It has been known for a long time that the late stage of MS is associated with marked atrophy of the brain. With increasing image quality and image processing methods, it has become evident that subtle atrophy is already present in the early phases of MS (Brex et al. 2000; Luks et al. 2000). The brain atrophy rate in MS is an important marker of disease progression and the atrophy rate in the first years of the disease seems to be a significant predictor of later disability status (Fisher et al. 2002). The atrophy proceeds through the course of MS, and most of the longitudinal studies have estimated atrophy rates of around 0.5% to 1% per year (Anderson VM et al. 2006; Bermel and Bakshi 2006) in MS patients, while brain volume loss in healthy controls is estimated to be 0.1% to 0.3% per year (Coffey et al. 1992; Pfefferbaum et al. 1994). The brain atrophy rate in MS seems to be independent of the disease subtype (Kalkers et al. 2002). The grey matter volume reduction in MS seems occur even in patients with minimal white matter lesion accumulation (Pagani et al. 2005) and it has been shown to be present from the earliest stages of the disease (Chard et al. 2002; Dalton et al. 2004; Sepulcre et al. 2006). White matter volume decreases in MS are rarely reported in the literature (Chard et al. 2002; Ge et al. 2001; Tedeschi et al. 2005). This might be a result of disease activity-related inflammation and oedema increasing the white matter volume and thereby masking the volume loss due to axonal degeneration (Dalton et al. 2004).

The corpus callosum (CC) is a typical site of MS lesions, and atrophy of the CC is commonly seen early in the course of MS (Audoin et al. 2007). CC atrophy has been shown to correlate with EDSS (Audoin et al. 2007) and cognitive impairment (Llufriu et al. 2012). The measure of the CC atrophy rate during the first year of DMT seems to be an accurate predictor of future disability accumulation (Vaneckova et al. 2012).

2.1.2. Treatment of MS

Currently there are no curative therapies available for MS. The aim of MS therapy in general is to shorten the duration of acute relapses, to reduce their frequency, and to thus provide relief of symptoms. Early initiation of the treatment can potentially reduce

the occurrence of relapses and subsequent development of disability (Clerico et al. 2008; Comi et al. 2001; Jacobs et al. 2000; Kappos et al. 2007). Traditional first-line treatment of MS includes IFN-β and GA. Also natalizumab and fingolimod, which are usually used as second-line therapies, can be used as a first-line treatment in cases of exceptionally aggressive disease (Elovaara 2012). Due to the significant but yet limited efficacy of first-line treatments, there is a substantial need for the development of new therapeutic agents for MS.

2.1.2.1. Disease-modifying therapies

The IFN-β drugs used in MS are naturally occurring cytokines secreted by immune cells. IFN-β has a wide variety of immunomodulatory activities (Hussien et al. 2001; Leppert et al. 1996; Sharief et al. 2001; Yong 2002; Yong et al. 1998). It also has antiviral activity, and this is the reason that IFN-βs were originally developed as therapeutic agents for MS (Borden et al. 2007). The IFN-β has been shown to reduce the amount of relapses by approximately one third, and they are recommended for RRMS patients who are intolerant to GA (Francis et al. 2001). Randomised, double-blind, placebo-controlled trials have shown that the use of IFN-β in MS patients reduced lesions visible in MRI by 50 to 80% (Li DK et al. 1999; Simon et al. 1998).

GA is a synthesised polypeptide mixture consisting of four different amino acids. In MS, GA is administered by subcutaneous injection. It has been shown to reduce the relapse rate by about one third, and to reduce lesion volume and the amount of Gd-enhancing lesions significantly (Comi et al. 2001). GA is recommended as a first-line treatment in RRMS patients and in patients who are intolerant to IFN-β drugs, or who have neutralising antibodies against IFN-β.

Natalizumab is a humanised monoclonal antibody administered intravenously once a month. In a pivotal phase III study, natalizumab treatment reduced the relapse rate 68% when compared to a placebo and reduced Gd-enhancing lesions during the second year by 92% and new or enlarging T2-lesions over 2 years by 83% (Polman et al. 2006). Despite being an efficient therapy against MS, natalizumab treatment has an important safety issue: an increased risk of an opportunistic infection caused by one type of human polyomavirus, John Cunningham virus (JCV) (Langer-Gould et al. 2005). This disease is called progressive multifocal leukoencephalopathy (PML), and often leads to death or several disability (Koralnik 2004). Prior use of immunosuppressants and increased duration of natalizumab treatment in combination with JCV seropositivity are factors which increase the risk of PML (Bloomgren et al. 2012). In addition, fingolimod has been shown to reduce relapse rate considerably, but it also has relatively rare but substantial adverse effects (Cohen et al. 2010).

2.1.2.2. Treatment of relapses

Intravenous or oral corticosteroids are typically used as treatment for acute relapses in MS patients. The exact mechanism of corticosteroids in MS is not completely clear. They have several modes of action, including reducing of oedema, stabilising BBB,

decreasing proinflammatory cytokines and inducing T cell apoptosis (Gold et al. 2001). Several studies have shown that the administration of high dose corticosteroids accelerates the recovery of disability caused by acute relapse, but does not have an influence on the final outcome after a relapse or the risk of subsequent relapse (Brusaferri and Candelise 2000; Miller DM et al. 2000). MRI studies have shown that the number of Gd-enhancing lesions decreases after corticosteroid treatment on acute relapse (Barkhof et al. 1991; Miller DH et al. 1992). Plasmapheresis is used as a second-line treatment in severe relapses that are not responding to corticosteroid treatment (Wiendl et al. 2008).

2.1.3. MS and pregnancy

During pregnancy, a wide variety of immunological and hormonal changes occurs, leading to downregulation of cell-mediated immunity and enhancement of humoral immunity (Coyle 2012).

Pregnancy modulates MS disease activity and typically stabilises the clinical course of the disease. Moreover, the onset of MS disease during pregnancy is unusual (Runmarker and Andersen 1995). During the third trimester, the relapse rate can be approximately 70% lower relative to the year before pregnancy (Confavreux et al. 1998). In contrast, aggravation of the disease is commonly seen soon after delivery. During the first three months after the delivery, the relapse rate is as much as 70% higher compared to the pre-pregnancy rate, and after that decreases to the pre-pregnancy level (Vukusic and Confavreux 2006; Vukusic et al. 2004). In spite of the common aggravation of MS soon after the delivery, pregnancy might have a favourable effect on the long-term outcome of MS (D'Hooghe et al. 2010; Runmarker and Andersen 1995). Furthermore, it has been shown that the number of pregnancies is inversely related to the first MS attack in CIS patients (Daumer et al. 2012; Ponsonby et al. 2012).

2.2 Fabry disease

FD is a rare X-linked metabolic disease first described by Fabry and Anderson in 1898. The incidence of FD has been estimated to be 1 per 111,700 live births (Spada et al. 2006). There are currently 44 patients (30 females, 14 males) with diagnosed FD in Finland (Kantola et al. 2012). FD is caused by a mutation in the GLA-gene in the X-chromosome leading to deficiency in the lysosomal enzyme, α-gal A. The error in α-gal A leads to accumulation of sfingolipids, especially globotriaocylceramide (Gb3), in cells. As a consequence, a multi-organ pathology occurs, most seriously affecting the kidneys, heart and cerebrovascular system (Clarke 2007; Zarate and Hopkin 2008). As an X-linked disease, FD affects all hemizygous males who have completely missing or minimal α-gal A activity and exhibit the classic phenotype (MacDermot et al. 2001). Most heterozygous females are also clinically affected, although there is more variability in α-gal A activity level and in the onset and disease severity than in hemizygous females (MacDermot et al. 2001; Whybra et al. 2009).

2.2.1. Clinical picture of FD

The first symptoms of FD emerge at between 3 and 10 years old in males and between 6 and 15 years old in females (Wilcox et al. 2008). However, especially in females, the diagnosis is often delayed at least three or even 20 years despite clinical symptoms and positive family history (Wilcox et al. 2008). The typical initial signs and symptoms of FD include neuropathic pain crises, angiokeratomas, hypohidrosis, and gastrointestinal problems, including diarrhoea, constipation, abdominal pain, nausea and vomiting (Ramaswami et al. 2006). FD patients typically present with major organ involvement in their 30s. Almost all male patients experience kidney dysfunction presenting first with mild proteinuria and progressing to loss of glomerular filtration rate (Schiffmann et al. 2009). Without ERT, end-stage renal disease is usually reached by the age of 40 in male FD patients (Ortiz et al. 2010; Ortiz et al. 2008). Cardiac manifestations are also common in FD. Typical cardiac complications in FD include left ventricular hypertrophy, valve thickening and conduction abnormalities (Kampmann et al. 2008). The major organ involvement together with other pathologies associated with FD leads to significant decrease in quality of life in both female and male patients. In male patients, FD typically reduces lifespan by approximately 15-20 years.

2.2.2. Brain MRI Findings in FD

The most typical finding on conventional MR scans is widespread progressive white matter lesions (WML) that are best detectable on T2 weighted images (Fellgiebel et al. 2006b; Moore et al. 2003; Reisin et al. 2011). Dolichoectasia has been reported to be a common finding in the intracranial arteries. The basilary artery (BA) diameter of stroke patients with FD has been shown to be significantly higher compared to stroke patients without FD, and the measure of BA may be a suitable screening tool in differential diagnosis of young patients with cryptogenic stroke (Fellgiebel et al. 2011). In addition, cerebral microbleeds have been shown to be relatively common, even among FD patients without a clinical history of cerebrovascular accident (Reisin et al. 2011). Symmetrical hyperintensity of the posterior thalami (pulvinar region) on T1-weighted images – the so-called pulvinar sign - is an almost pathognomonic finding in FD. However, the sensitivity of the pulvinar sign is weak. Burlina et al. (2008) found the pulvinar sign in 25% of male FD patients, but none of their 43 female FD patients showed this finding.

2.2.3. Enzyme replacement therapy in FD

Currently, two forms of ERT are available for the treatment of FD: Agalsidase alfa (Replagal, Shire Human Genetic Therapies, Inc., Cambridge, MA, USA) and agalsidase beta (Fabrazyme, Genzyme Corporation, Inc., Cambridge, MA, USA). Agalsidase alfa is produced in a human cell line by gene activation. Agalsidase beta is produced in Chinese hamster ovary cells. Both of these preparations are administered intravenously every other week (Schiffmann et al. 2001). Based on the studies available, it cannot be concluded whether one of the ERT preparations is better than the other. A randomised study with an 18-month following time showed no difference in

treatment effects between agalsidase alfa and agalsidase beta (Sirrs et al. 2009). There are numerous studies on the effect of ERT in FD. The reports strongly support the clinical benefit with ERT, although there is considerable variation in the response to ERT, probably due to variation in the phenotypic expression in patients with FD. In a randomised, double-blind, placebo-controlled trial, agalsidase-beta therapy slowed progression of renal, cardiac and cerebrovascular complications compared with the placebo in patients with advanced FD (Banikazemi et al. 2007). ERT has also been shown to reduce symptoms and to improve quality of life in FD patients (Parini et al. 2008).

2.3 MRI

MRI is the method of choice for imaging diseases affecting the CNS. MR offers superior tissue contrast compared to computed tomography and is free of artefacts caused by bony structures. A significant additional advantage of MRI is that no ionising radiation is needed. Longer scanning times are a disadvantage of MRI and makes it susceptible to motion artefacts. Contraindications to MRI include cardiac pacemakers, cochlear implants, implanted neurostimulators, older ferromagnetic aneurysm clips and metal in the eye (Shellock et al. 1993).

2.3.1 Diffusion-weighted imaging

DWI utilises the random thermal motion of water molecules, also known as Brownian motion. In DWI, a conventional MR sequence is modified by adding two additional gradient pulses. These two pulses are strong and symmetrical in relation to a 180˚ rephasing radio frequency (RF) pulse. The first gradient pulse dephases the spins of water molecules and, if the water molecules were completely immobile, the second gradient pulse rephases these spins. When the water molecules move in the direction of the diffusion gradients during the time interval between the applications of the two gradients, the rephasing effect by the second gradient pulse remains imperfect and causes signal attenuation that depends on the level of diffusion within a voxel. The amount of signal attenuation can be calculated as

e^{-bD},

where D is the diffusion coefficient within a tissue and the b-factor indicates the amount of diffusion weighting of the diffusion imaging sequence. The b-factor depends on the timing and strength of the diffusion gradients and is determined by the following relationship:

$b=\gamma^2G^2\delta^2(\Delta-\delta/3)$,

in which γ is the gyromagnetic ratio for hydrogen nucleus; G is the magnitude and δ is the duration of the diffusion gradient, and Δ the time between the centres of the two diffusion gradients (Le Bihan et al. 2001).

If pure diffusion, which is not hindered by any physical obstacle, is measured, D can properly summarise the diffusion of water molecules. On the contrary, in a biological system where the diffusion is affected by multiple factors, another term is used: the "apparent" diffusion coefficient (ADC) (Beaulieu 2002).

The signal of the diffusion-weighted image depends on both T2 signal intensity and the level of diffusion:

$S_1 = S_0 \times e^{-bD}$,

where S_1 is the diffusion-weighted signal and S_0 is the signal at the same voxel without the addition of the diffusion-sensitising gradients (b=0). Hence, a high signal on DWI may be related not only to reduced diffusion but also to T2 prolongation (T2 shine-through). When DWI imaging is acquired with at least 2 different b-values, ADC maps can be calculated. When hyperintense areas on DW images are seen, the ADC maps must be surveyed along with the DW images to distinguish between T2 prolongation and diffusion restriction.

The diffusion distance of a water molecule decreases in an anisotropic environment, such as brain tissue. This restriction of diffusion is caused by obstacles which are formed by surrounding structures such as membranes and cell organelles.

The sensitivity of one diffusion-weighted sequence is limited to diffusion in the direction of the gradients. Therefore, it must be repeated in 3 orthogonal directions to obtain the image weighted in global diffusion (trace image).

Diffusion-weighted imaging can be performed using several different types of sequence. Diffusion-weighted sequences are highly sensitive to macroscopic motion, for example due to patient motion or vascular pulsations. The most widely used technique is the diffusion-weighted single-shot echo-planar imaging sequence (DW-EPI) (Turner et al. 1990). The very fast read-out makes DW-EPI less vulnerable to motion artefacts. On the other hand, echo planar imaging is prone to artefacts caused by susceptibility and magnetic field homogeneity variations. Another drawback is the weak spatial resolution due to the rapid T2* decay which occurs during the acquisition of the gradient echo train.

DWI is clinically used on daily basis. It is a very sensitive tool in modern neuroimaging for detecting acute brain ischemia (Harris et al. 2009). It is also useful in the evaluation of brain tumours (Gerstner and Sorensen 2011) and detecting brain infectious conditions (Ebisu et al. 1996; Tung and Rogg 2003) and diffuse axonal injury, especially in the acute setting (Liu AY et al. 1999).

2.3.2 Diffusion tensor imaging

DTI is an advanced form of DWI, in which the gradients must be applied in at least six different directions, which makes it possible to create a mathematical model of diffusion in three-dimensional space, known as the diffusion tensor (Alexander et al.

2007; Mukherjee et al. 2008). From this measured tensor, it is possible to calculate the principal eigenvalues, which are annotated as 1, 2 and 3, in order of largest to smallest magnitude of diffusivities (Neil 2008; Nucifora et al. 2007) and their orientations, called eigenvectors (Pierpaoli and Basser 1996). The eigenvector having the largest eigenvalue reflects the diffusion parallel to the axonal fibres and is also called axial diffusivity (AD). The two smaller eigenvectors are orientated perpendicular to the axonal fibres. The average of the eigenvalues of these two smaller eigenvectors is the radial diffusivity (RD). The average of all three eigenvalues is the mean diffusivity (MD).

Several different parameters are obtainable from DTI images. The most commonly used diffusion parameter is FA, which is a measure of the magnitude of anisotropic diffusion with values ranging from 0 to 1 (Le Bihan et al. 2001). For isotropic diffusion, the diffusivities are the same in all directions and FA equals 0. In a theoretical case where the diffusion only occurs in one direction (i.e. the second and third eigenvalues equal 0), FA reaches its maximal value of 1. FA values are independent of the frame of reference, of the direction of the applied diffusion gradients, and of the direction of the tissue structures within each voxel (Basser et al. 1994).

2.3.3. Methods of analyzing MRI data

2.3.3.1. Region of interest-based methods

One way to analyse DWI or DTI derived images is to manually fit region of interests (ROI) to selected brain regions and measure parameter values within the ROIs (Bester et al. 2008; Lin et al. 2008; Wu et al. 2009). The ROIs are usually located on the basis of b0 images, the direction-coded anisotropy maps or conventional sequences obtained at the same imaging session as the DWI imaging (Bartha et al. 2007; Counsell et al. 2006; Provenzale et al. 2007; Saksena et al. 2008). The ROI method is an operator-dependent method; the accuracy of positioning of the ROIs is based on the anatomical knowledge of the researcher performing the measurements. There is regional variability in the reproducibility of ROI-based DTI measurements (Marenco et al. 2006; Ozturk et al. 2008). The reproducibility of ROI-based measurements seems to be best in areas which can be delineated precisely, such as the internal capsule, whereas other areas, especially in the vicinity of CSF spaces, are much more challenging (Lepomäki et al. 2012).

2.3.3.2. Histogram-based methods

ADC histogram analysis has been shown to be a robust and reproducible method (Steens et al. 2004). Histogram-based methods have been frequently used in analysing DWI derived data in MS (Cercignani et al. 2001; Sämann et al. 2012). This method has been used for the whole brain tissue after extracting CSF from the images. There are also tools to extract visible brain lesions and to segment grey and white matter to

separate volumes. Hence, histogram analysis can also be performed for normal appearing white (NAWM) or grey matter (NAGM) (Oreja-Guevara et al. 2005; Rovaris et al. 2002). Magnetization transfer (MTR) histogram analysis of the brain of MS patients has also been used (Catalaa et al. 2000; Fernando et al. 2005).

The advantage of the histogram method compared to ROI-based methods is that it is not operator dependent. Furthermore, with histogram analysis, the three-dimensional diffusion information of the entire brain can be reduced to a single number used for intersubject comparisons. On the other hand, histogram analysis does not produce any spatial information on possible abnormalities in the brain studied, and possible small regional areas with modest diffusion abnormalities may have such small impact on the global whole brain diffusion parameters that they might be missed with histogram analysis (Oreja-Guevara et al. 2005).

2.3.3.3. Tract-Based Spatial Statistics

Tract-Based Spatial Statistics (TBSS) is a voxel-based method having advantages over ROI-based on histogram-based methods: it is not user dependent and it can reveal regional white matter abnormalities of DTI parameters on a group level. In TBSS, two or more groups of study subjects are compared and the DTI data are projected onto an "FA skeleton" which is common to all subjects participating the study (Smith et al. 2006; Smith et al. 2007a).

TBSS has been widely used in studies of different diseases, such as mild cognitive impairment and Alzheimer disease (Liu YW et al. 2011), Lewy body disease (Watson et al. 2012), temporal epilepsy (Afzali et al. 2011), MELAS (mitochondrial encephalomyopahty, lactic acidosis and stroke-like episodes) (Virtanen et al. 2011) and pathological gambling (Joutsa et al. 2011). TBSS has also been used to measure white matter maturation of preterm infants (Lepomäki et al. 2013).

TBSS is provided by FMRIB (http://www.fmrib.ox.ac.uk/fsl/). It includes the following steps: All of the subject´s FA images are aligned to common registration target using nonlinear registration (Andersson et al. 2007a; b). Then, a mean FA image is built based on all of the subject´s aligned FA images. The mean FA image is thinned to create a mean FA skeleton that represents the centres of all of the tracts common to all subjects. Each subject´s aligned FA images are then projected onto the mean FA skeleton and the resulting data can be fed into voxelwise cross-subject statistics. With TBSS, the voxelwise analysis can also be performed for any other DTI parameter data by applying nonlinear registration to the data which is then projected onto the mean FA skeleton (Smith et al. 2006). The FA data is then used to find the projection vectors for voxelwise analysis of the desired DTI parameter.

2.3.3.4. Brain volume measurements

Volumetric brain MR imaging has been an important part of neuroimaging studies for almost as long as MR imaging has been available. Volumetry has been widely used not

only in neurodegenerative disorders such as Alzheimer disease (Mueller et al. 2010), MS (Kalincik et al. 2012), frontotemporal dementia and amyotrophic lateral sclerosis (Lillo et al. 2012), but also in many other conditions, e.g. schizophrenia (Iwashiro et al. 2012), epilepsy (Farid et al. 2012), MELAS (Virtanen et al. 2011) and narcolepsy (Brabec et al. 2011).

When whole brain volumes are measured, the absolute volume measurements are not comparable between different subjects because of the variation of the size of the cranium between individuals. One option for standardising the brain volume measurements is computation brain volume index (BVI), dividing brain volume (intracranial volume-CSF volume) by intracranial volume (Mascalchi et al. 2004). Nowadays, automated algorithms for the normalisation of brain volumes have been developed.

Structural Image Evaluation using Normalization of Atrophy (SIENA) and its adaptation for cross-sectional measurements (SIENAX) (Smith et al. 2001; Smith et al. 2002) are widely used, fully automated whole brain atrophy algorithms provided by FSL (Smith et al. 2004). SIENAX measures the volume of the brain from a single MRI and is useful for cross-sectional studies, whereas SIENA measures the percentage brain volume change (PBVC) between two scans of the same subject and has been developed for longitudinal studies (Smith et al. 2007b).

In SIENA, after extracting the brain and skull images from the single whole-head input data (Smith 2002), the two brain images of the same subject are aligned to each other (Jenkinson et al. 2002; Jenkinson and Smith 2001); both brain images are resampled into the space halfway between the two. Then, a tissue-type segmentation is performed to find the brain/non-brain edge points, and perpendicular edge displacement between the two time points is estimated. The final step in SIENA is the conversion of the mean edge displacement into a global estimate of PBVC between the two timepoints.

SIENAX starts by extracting the brain and skull images from the single whole-head input data (Smith 2002). These are then registered to the Montreal Neurologic Institute 152 (MNI 152) (Jenkinson et al. 2002; Jenkinson and Smith 2001) space using the skull image to determine the registration scaling. The final step in SIENAX is the tissue-type segmentation procedure (Zhang et al. 2001) and estimation of total brain tissue volume, gray matter volume and white matter volume.

FMRIB´s Software Library´s (FSL) optimised tool for voxel based morphometry style analysis (FSL-VBM) (Douaud et al. 2007; Good et al. 2001) is used to perform voxel-wise comparisons of the local volume of grey matter in different brain regions between two groups of study subjects.

FSL-VBM starts by extracting the brain tissue from the original images (Smith 2002), after which a tissue-type segmentation (Zhang et al. 2001) producing grey matter partial volume images is performed. The resulting data is then aligned to MNI-152 space using the affine registration tool, FMRIB´s Linear Image Registration Tool (FLIRT) (Jenkinson et al. 2002; Jenkinson and Smith 2001), followed by nonlinear registration using FMRIB´s Nonlinear Registration Tool (FNIRT) (Andersson et al.

2007b), which uses a b-spline representation of the registration warp field (Rueckert et al. 1999). These images are then averaged to create a study-specific template, to which the native grey matter images are non-linearly re-registered. The registered partial volume images are then modulated to correct for local expansion or contraction. These data are then smoothed with an isotropic Gaussian kernel with an appropriate sigma value. The resulting data can be used for voxelwise testing of differences of local grey matter volumes between study groups.

Results obtained with FSL-VBM have been shown to correlate strongly with another VBM-style analysis, SPM-VBM (based on Statistical Parametric Mapping software package) (Battaglini et al. 2009). FSL-VBM has been used to study MS (Bendfeldt et al. 2010), vascular dementia (Li CM et al. 2011), attention-deficit/hyperactivity disorder (Seidman et al. 2011) and restless legs syndrome (Rizzo et al. 2012).

3. AIMS OF THE PRESENT STUDY

The general aim of this study was to explore the usefulness of brain MRI, DWI and DTI in monitoring MS activity and to reveal brain tissue changes in FD at 1.5 T.

The more specific aims were:

I To evaluate whether MRI and DWI could reveal early activation of MS during the post-partum period by longitudinal MRI and DWI follow-up of pregnant RRMS patients.

II To evaluate what kinds of change take place in the brain white matter of pregnant RRMS patients.

III To evaluate what kinds of change take place in the brain white matter of patients with newly diagnosed RRMS having disease-modifying treatment.

IV To reveal possible disturbances of white matter integrity of patients affected by Fabry disease by using voxelwise analysis of DTI parameters.

Note: The roman numerals refer to the original publications

4. SUBJECTS AND METHODS

4.1. MS studies (Studies I, II and III)

4.1.1. MS patients and clinical follow up

4.1.1.1. Pregnant MS patients (Studies I and II)

Study I included 28 and Study II 19 pregnant patients with RRMS. The characteristics of the patients in studies I and II are displayed in Table 1. Patients were clinically and radiologically examined in the University hospitals of Turku (11 patients in both studies), Helsinki (12 patients in Study I, 8 patients in Study II) and Tampere (5 patients in Study I). The majority of the patients joined the study during the first trimester of pregnancy and they were followed up for 6 months post-partum with recording of relapses. Neurological examinations were performed at 10-12 and 26-28 weeks of gestation and 4-5 weeks and 6 months post-partum with assessment of disability by EDSS and recording of relapses. The pregnant patients examined in Study I were also included in Study II with the following exceptions: the 5 patients examined in Tampere were excluded because of the lack of diffusion-weighted images; 4 patients examined in Helsinki were excluded because the DWI images were not technically sufficient to produce a proper ADC map.

MRI presents no known risk to the foetus during pregnancy (Baker et al. 1994; Myers et al. 1998; Reeves et al. 2010). However, during the first trimester, MRI is recommended only when it is considered necessary for the mother´s health (http://www.valvira.fi/files/tiedostot/l/h/LH-2000-1_magneettitutkimukset.pdf). Our interest was to obtain MRI images during the third trimester, which is known to be clinically the most stable period of pregnancy in MS (Vukusic et al. 2004). The scans were focused mainly on the beginning of the third trimester for the convenience of the patients. For the same reason, the post-partum scans were not performed sooner than 4 weeks after the delivery. The study was approved by the ethical committee of the Turku University Hospital, and a written informed consent was obtained from all subjects.

Table 1. MS patients characteristics in studies I and II. EDSS, Expanded Disability Status Scale; SD, standard deviation.

No. of patients	
Study I	28
Study II	19
Age at onset of pregnancy (years; mean ± SD)	
Study I	30.2 ± 3.9
Study II	31.6 ± 4.6
Duration of disease at onset of pregnancy (years; mean ± SD)	
Study I	5.4 ± 4.1
Study II	5.9 ± 4.4
Number of relapses before the study onset (mean ± SD)	
Study I	3.8 ± 2.1
Study II	4.3 ± 2.4
EDSS at 3rd trimester	
Study I	1.2 ± 1.1
Study II	1.3 ± 1.0
EDSS at 6 months post-partum	
Study I	1.5 ± 1.2
Study II	1.4 ± 1.2

4.1.1.2. Non-pregnant MS patients with newly diagnosed MS (Study III)

Nine (eight women, one man) MS patients were included in Study III. All of them had newly diagnosed RRMS and had experienced two or three relapses during the year preceding the study (mean number of relapses ± standard deviation [SD] was 2.33 ± 0.5). The mean age of the patients was 32.4 years (SD 6.3 years, range 23-42 years). All patients started IFN-β therapy. All patients were neurologically examined, including assessment of EDSS, both before and three months after initiation of treatment. Mean EDSS was 1.56 (SD 0.81, range 1.0-3.5) at the beginning of the study and 1.72 (SD 0.94, range 1.0-3.5) at the end of the clinical follow-up. The patient characteristics are shown in Table 2.

Table 2. Demographic and clinical data and number of new T2-lesions in the imaging performed 3-4 months after initiation of interferon beta treatment.

Pat. nro	Age/sex	New T2(1	EDSS(2	Relapses before/follow-up(3	Delay from relapse to MRI(4
1	37 f	0	2.0/2.0	2/1	2
2	38 f	0	1.0/1.0	2/1	5
3	27 f	0	1.5/1.0	3/0	2
4	42 f	0	1.5/1.5	2/0	1
5	23 f	4	1.0/1.0	3/1	7
6	37 f	2	1.5/1.5	2/1	2.5
7	28 f	1	1.0/1.0	2/0	6
8	32 f	9	1.0/3.0	3/1	1
9	28 m	6	3.5/3.5	2/1	4

1) Number of new T2 lesions in the second MRI
2) EDSS before and three months after initiation of the treatment
3) Number of relapses during one year preceding the initiation of the treatment and during the first year of the treatment
4) Number of months between the last relapse and the first MRI

4.1.2. Timing and image acquisition protocol of MRI (Studies I, II and III)

In Study I, a maximum of four serial MR examinations were performed. Every patient was scanned at least once during pregnancy and once post-partum. The mean time interval between the imaging performed during pregnancy (if imaged twice, the last imaging date) and post-partum (if imaged twice, the first imaging date) was 15.6 weeks (range 7-25 weeks). All scans performed during pregnancy were performed during the third trimester. Five patients were scanned twice during the third trimester. All post-partum scans were performed within 12 weeks of delivery; the majority (23, or 82%) within six weeks. Four patients were scanned for a second time post-partum between weeks 10 and 12.

In Study II, one pre-partum and one post-partum imaging of all 19 patients were included. If imaging was performed twice pre- or post-partum, the first image was included in the study. Hence, all included pre-partum images were obtained between weeks 25 and 28 and the post-partum images between weeks 4 and 7, apart from one patient who was imaged 10 weeks post-partum. The timing of MR scans related to the gestational and post-partum weeks in Studies I and II is illustrated in Figure 1. The mean time interval between the pre- and post-partum imaging was 18 weeks (range 12-25 weeks) in Study II.

Figure 1. The timing of MRI during pregnancy and postpartum in studies I and II. Tku, Turku; Hki, Helsinki; Tre, Tampere

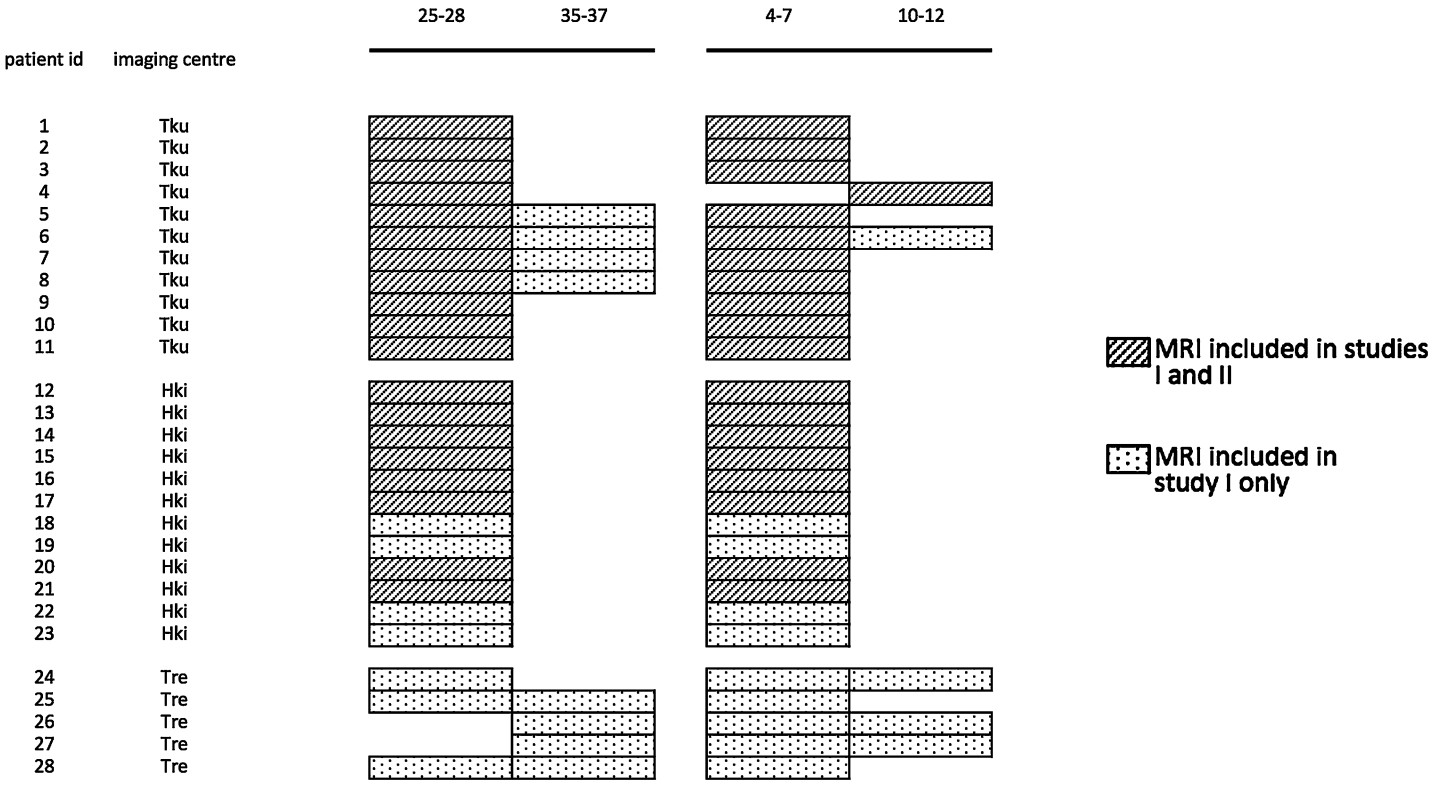

In Study III, all patients were studied twice by MRI. The first MRI was performed immediately before initiation of IFN-β treatment and the second about three months after the initiation of the treatment. The mean time interval between the first and second imaging was 103 days (range 84-125 days).

MRI imaging for Study I was performed in three different imaging centres (Helsinki, Turku and Tampere). The field strength of each scanner was 1.5T (Helsinki: Magnetom Vision, Siemens, Erlangen, Germany; Turku Gyroscan Intera, Philips, Best, The Netherlands; Tampere Genesis Signa, GE Medical Systems, Milwaukee, USA). The same image material, with the above-mentioned exceptions, was used in Study II. The patients imaged in Study III were scanned in Turku with the same scanner used in Studies I and II.

T2-weighted sequences with 5-mm transverse slices (scanning parameter ranges: repetition time [TR], 3696 – 5060 msec; echo time [TE], 90 – 126 msec; 1mm interslice gap) were obtained from the foramen magnum to vertex. T1-weighted scans (TR, 560 – 660 msec; TE, 12 – 15 msec) were obtained in the same scan plane, thickness and position as the T2 scans. Gd-enhanced T1-weighted sequences with scanning parameters, slice thickness and patient position identical to the non-enhanced T1-weighted sequence were obtained in all post-partum scans performed in Turku and in one post-partum scan performed in Tampere, and also in all of the scans included in Study III. Fluid-attenuated inversion recovery (FLAIR) sequences (scanning parameter ranges: TR, 9002 - 11000 msec; TE, 105 - 187 msec; inversion time [TI], 2200 – 2500 msec) with 5-mm contiguous slices were obtained in the sagittal plane. In the scans performed in Helsinki and Turku multislice diffusion-weighted images (DWI) were obtained with echo planar imaging (TR/TE 4000-4666/86-139 msec; b values: 0 and 1,000 s/mm^2 in Turku; 50, 500 and 1000 s/mm^2 in Helsinki) in the axial plane with slice thickness of 5 mm and interslice gap of 1 mm. All axial slices were arranged in parallel on the line between the inferior margin of the splenium and the genu of the corpus callosum.

4.1.3. Image analysis (Studies I, II and III)

4.1.3.1. MS lesion load recording (Studies I, II and III)

Lesions appearing in T2-weighted images as new or enlarging when compared with a pre-existing scan were considered to be “active lesions”. A sagittal FLAIR scan was used to increase confidence in lesion identification. White matter lesion total volumes were determined from sagittal FLAIR scans using a semiautomated thresholding technique using Advantage Workstation (v.3.1.) software installed on a SUN workstation (SUN Microsystems). The FLAIR sequence was chosen for lesion volume measurement because of its convenience in assessing intensity limits of separate MS lesions having high signal compared to normal appearing brain tissue and especially of CSF having no signal in the FLAIR sequence. From the diffusion trace images, with a b-value of 1000 s/mm^2, lesions appearing as clearly hyperintense related to normal appearing white matter were calculated and considered to be “DWI-positive” lesions in

Study I. ADC maps were inspected alongside with diffusion-weighted images to detect possible lesions with diffusion restriction (Fig. 2). From each MRI the numbers of T1-hypointense were also registered. Both "black holes" and lesions having lower intensity than NAWM but higher intensity than CSF were included in T1-hypointense lesions. Also the enhancing lesions were counted, when Gd was used.

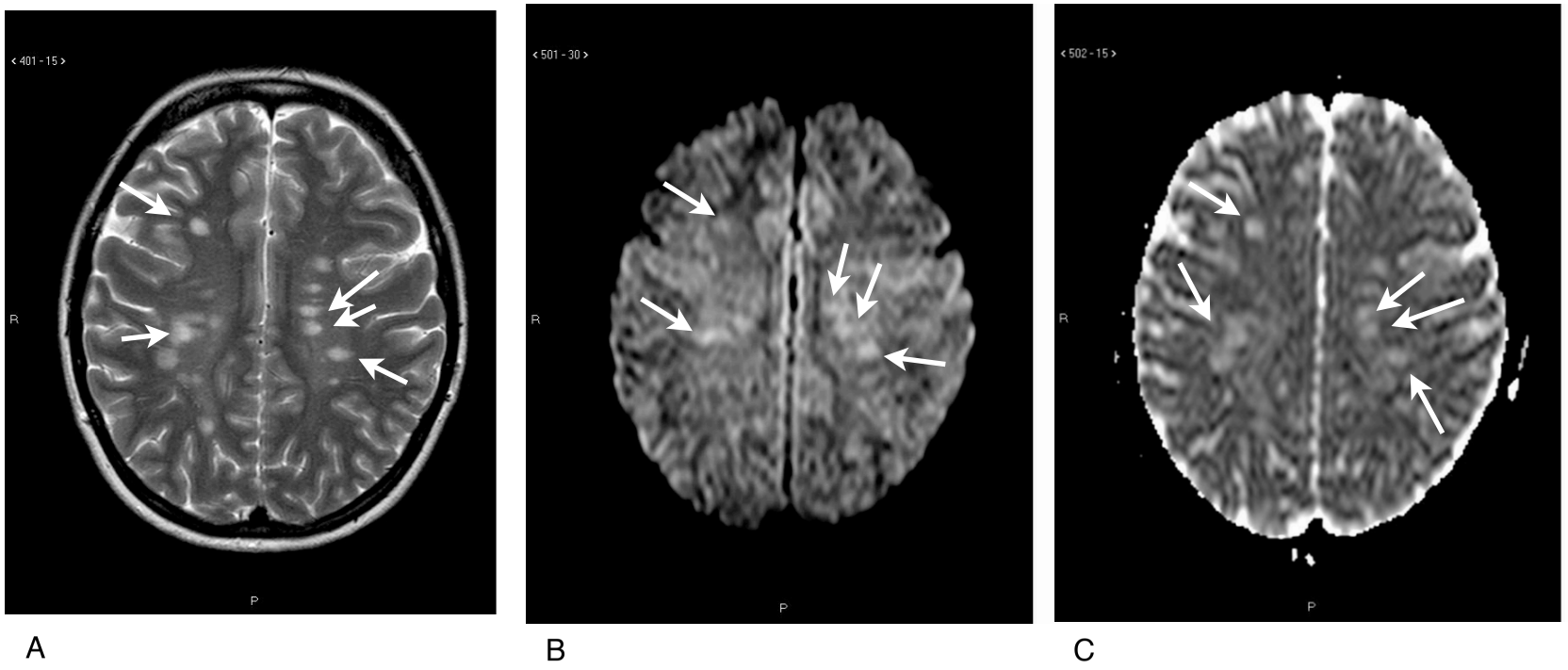

Figure 2. Pregnant patient with MS having several lesions in the centrum semiovale in T2-weighted images (A). Many of these lesions appear bright on diffusion-weighted image with b-value of 1000 s/mm^2 (B). In the ADC map (C), the corresponding lesions appear bright, consistent with elevated ADC. Hence, the high signal in diffusion-weighted images is due to T2 shine-through, but not diffusion restriction.

4.1.3.2. Segmentation, histogram analyses and brain volume analyses (Studies II and III)

4.1.3.2.1 Study II

Brain tissue was first segmented from non-brain tissue by using the Brain Extraction Tool (BET), part of FSL 4.1 (Smith 2002). Then, to segment brain parenchyma from CSF, for each b_0 image we created a binary brain mask by using the FMRIB's Automated Segmentation Tool (FAST 4.1, part of FSL 4.1) 2-class segmentation function (Zhang et al. 2001). This mask was applied to the ADC maps using the fslmaths tool (part of FSL 4.1) for voxel-by-voxel data extraction. ADC histograms with 256 bins were generated using the fslstats tool (part of FSL 4.1). After normalisation for brain volume, the mean and peak positions of the whole-brain ADC-histograms were computed using the Prism software, Version 5 (Graph Pad software, San Diego, California).

Brain volumetry was performed by measuring the PBVC on the T1 images with SIENA (Smith et al. 2001; Smith et al. 2002), part of FSL 4.1 (Smith et al. 2004). SIENA starts by extracting brain and skull images from the two-timepoint whole-head input data (Smith 2002). The two brain images are then aligned to each other (Jenkinson et al. 2002; Jenkinson and Smith 2001) (using the skull images to constrain the registration scaling); both brain images are resampled into the space half way between the two. Next, tissue-type segmentation is carried out (Zhang et al. 2001) in order to find the brain/non-brain edge points, and then perpendicular edge displacement (between the two timepoints) is estimated at these edge points. Finally, the mean edge displacement is converted into a (global) estimate of PVBC between the two time points.

4.1.3.2.2. Study III

The ADC-map post-processing was performed using the method previously described by Mascalchi et al. (2002), and included the following steps: manual segmentation of the extracranial tissues; application of a threshold value of 2.39×10^{-3} mm^2/s to separate brain from pixels containing CSF; and computation of whole-brain ADC histograms. The lower quartile, median, upper quartile, mean and peak positions were determined from the ADC histograms. BVIs were calculated by dividing the brain volume by the sum of brain volume and CSF volume.

4.1.4. Statistical analysis (Studies I, II and III)

A paired two-tailed Student´s t-test was used to compare annualised relapse rates and EDSS values at different time points in Studies I and II. To compare the ADC values (Studies II and III) and the number and volume of the lesions (Studies I,II,III) during and after pregnancy, the Wilcoxon matched-pairs signed-ranks test was used. The Mann-Whitney U test was used to determine the difference in ADC histogram parameter change (magnitude) between patients with and without active MS lesions in

Study III.

To correlate the percentage mean ADC change (ADC%) with PBVC and percentage lesion volume change (VOL%), the Spearman rank correlation coefficient was calculated in Study II. The associations between the number of new T2-lesions and ADC parameter changes (magnitude) in Study III were also calculated using the Spearman rank correlation coefficient.

4.2. Fabry disease (Study IV)

4.2.1. FD patients

Study IV included 12 clinically affected FD patients (mean age, 39 years; range 16-68 years; 4 men, 8 women) and 13 healthy controls (mean age, 46 years; range, 32-66 years; 2 men, 11 women). Diagnosis was confirmed by genetic analysis. The mutation was not found in one patient. However, this female patient was an obligate carrier with typical clinical findings and missing α-gal A activity. One patient (male, at age 48) had undergone renal transplantation because of end-stage renal failure caused by FD. At the time of MRI, 7 patients (58%) were receiving ERT (agalsidase beta) (mean duration of ERT=4.5 years, range=4.1 – 6.1 years). The demographic characteristics of all of the patients are shown in Table 3.

Table 3. Demographic characteristics of Fabry disease patients.

			Fabry disease manifestations				
Patient number	Age/years	Duration of ERT[a]/years	Neuropathic pain	Angiokeratoma	Cardiac dysfunction[b]	Renal dysfunction[c]	Stroke/TIA
Females							
1	68	4.3	+	-	+	+	-
2	61	4.3	+	-	+	+	-
3	48	4.4	+	-	+	-	-
4	47	-	-	+	+	+	-
5	46	4.3	+	-	+	-	+
6	32	-	-	+	+	+	-
7	19	-	+	+	-	-	-
8	16	-	+	+	-	-	-
Males							
9	54	4.2	+	+	+	+	-
10	31	6.1	+	+	-	-	-
11	24	4.1	+	+	+	-	-
12	17	-	-	+	-	-	-

[a]Duration of enzyme replacement therapy at the time point of MR imaging
[b]Including arrhythmias, left ventricular hypertrophy, cardiomyopathy
[c]Including proteinuria, renal insufficiency

4.2.2. MRI protocol

The imaging protocol for conventional MR images included an axial T1-weighted 3D (TR, 25 ms; TE, 4.6 ms; flip angle 30°, slice thickness 1.6 mm, spacing 0.8 mm) sequence, axial T2-weighted (TR, 4438 ms; TE, 100 ms, slice thickness 5.0 mm, spacing 6.0 mm) sequence and coronal FLAIR (TR, 11000 ms; TE, 140 ms; TI 2800 ms, slice thickness 5.0 mm, spacing 6.0 mm) sequence. DTI data were collected using a single-shot echo-planar imaging sequence (TE=89 ms, TR=5451-5616 ms) with 16 gradient-encoding directions, a section thickness of 3 mm and an intersection gap of 1 mm. The DTI data were obtained with a matrix size of 112 X 112. The b-values used for diffusion weighting were 0, 600 and 1200 s/mm^2.

4.2.3. Image analysis

4.2.3.1. Conventional MR image analysis

The WML load was rated according to a modified Fazekas scale by an experienced neuroradiologist, who was blinded to the clinical data of the study subjects. The original Fazekas (Fazekas et al. 1987) classification on WML severity has been shown to reflect different aetiologies of MRI signal abnormalities. Hyperintense caps and a smooth halo around the lateral ventricles seem to be of nonischemic aetiology (Fazekas et al. 1993). Therefore a modified Fazekas score (mFs) was used (Andréll et al. 2005). Accordingly, WML load severity was graded with a scale ranging from 0 to 3 (0=absence of WMLs; 1=punctate foci; 2=beginning confluence of lesions; 3=large confluent areas). An mFs of 0 or 1 was considered a "mild" burden of WML and an mFs of 2 or 3 was considered a "severe" burden. In addition, the presence of lacunar or cortical infarctions was registered.

4.2.3.2. DTI data analysis

DTI data analysis was carried out following the standard procedure of voxelwise cross-subject analysis using TBSS (Smith et al. 2006). First, the raw diffusion data were corrected for eddy current-induced distortions. The FA, MD and eigenvector maps were calculated using the FMRIB´s Diffusion Toolbox (FDT) program. The first eigenvector corresponds to axial diffusivity (AD). A measure of radial diffusivity (RD) was produced with fslmaths by calculating the average of the second and third eigenvectors of each voxel. Automatic brain extraction was performed for the resulting maps using BET (Smith 2002). The FA data for all of the subjects were then aligned into a common space using FNIRT (Andersson et al. 2007a; b). Next, a mean FA image was created and thinned to create a mean FA skeleton representing the centres of all of the tracts common to the group. The threshold of the mean FA skeleton was set at 0.2. Each subject´s aligned FA images were then projected onto the mean FA skeleton and the resulting data fed into voxelwise cross-subject statistics.

Voxelwise cross-subject TBSS analysis for the MD, AD and RD data was performed

by applying nonlinear registration to the corresponding DTI parameter maps, which were then projected onto the original mean FA skeleton. The FA data were used to find the projection vectors for the voxelwise MD, AD and RD analyses.

We performed voxelwise cross-subject TBSS-analysis for FA and MD to compare all 12 patients and 13 controls. Voxelwise cross-subject analysis for FA and MD was also performed to compare patients receiving ERT (mean age, 47 years; range, 24 to 68 years; 3 men, 4 women) with patients without ERT (mean age, 26 years; range, 16 to 47 years; 1 man, 5 women). Both of these analyses were performed using age and gender as covariates.

Guided by the TBSS findings, we performed a ROI analysis for the 8 FD patients having a mFs of 0 or 1. Eight healthy controls with an mFs of 0 or 1 were also chosen for ROI analysis (Table 4). The ROI analysis was performed for the each subject's FA, MD, AD and RD skeletons using one large ROI mask containing all of the voxels showing significant FA reduction in FD patients. We also performed separate TBSS analyses for FA, MD, AD and RD for these 8 FD patients and 8 controls with mFs 0 or 1. Age and gender were also used as covariates in these analyses.

Table 4. White matter lesion load, age and gender of study subjects in DTI analyses. mFs, modified Fazekas score.

TBSS ANALYSIS						
	FD patients			Controls		
mFs[a]	number	age (mean ± SD)	female/male	number	age (mean ± SD)	female/male
0	5	23.0 ± 7.8	3/2	6	38.7 ± 5.5	6/0
1	3	43.8 ± 18.6	2/1	6	51.2 ± 8.5	5/1
2	3	56.8 ± 10.0	2/1	1	60.9	0/1
3	1	46.4	1/0	0		
total	12	38.6 ± 17.8	8/4	13	46.2 ± 10.1	11/2
ROI ANALYSIS						
	FD patients			Controls		
mFs[a]	number	age (mean ± SD)	female/male	number	age (mean ± SD)	female/male
0	5	23.0 ± 7.8	3/2	5	37.6 ± 5.4	5/0
1	3	43.8 ± 18.6	2/1	3	47.2 ± 6.7	2/1
total	8	30.8 ± 15.8	5/3	8	41.2 ± 7.4	7/1

4.2.3.3. Volumetry

The brain tissue volumes of the study subjects, normalised for subject head size, were estimated using SIENAX (Smith et al. 2001; Smith et al. 2002). First, brain tissue was extracted from the original 3D T1-weighted images using BET (Smith 2002). The extracted brain images were then affine-registered to standard (Montreal Neurologic Institute 152, Montreal, Quebec, Canada) space (MNI152) (Jenkinson et al. 2002; Jenkinson and Smith 2001). The final step was a tissue-type segmentation procedure (Zhang et al. 2001), producing estimates of total brain tissue volume, grey matter volume and white matter volume.

We used FSL´s voxel-based morphometry style analysis (FSL-VBM) (Ashburner and Friston 2000; Good et al. 2001) to analyse regional differences in grey matter volume. After extracting the brain tissue from the original 3D T1-weighted images with BET (Smith 2002), tissue-type segmentation (Zhang et al. 2001) producing grey matter partial volume images was performed. The resulting data were then aligned to MNI-152 space using FLIRT (Jenkinson et al. 2002; Jenkinson and Smith 2001), followed by nonlinear registration using FNIRT (Andersson et al. 2007a; b), which uses a b-spline representation of the registration warp field (Rueckert et al. 1999). These images were then averaged to create a study-specific template, to which the native grey matter images were then non-linearly re-registered. The registered partial volume images were then modulated to correct for local expansion or contraction. These data were then smoothed with an isotropic Gaussian kernel with a sigma of 3 mm. The resulting data were used for voxelwise testing.

4.2.4. Statistical analysis

A two-tailed unpaired t-test was used to analyse the difference in brain volumes between the FD patients and the controls. The two-tailed unpaired t-test was also used in the ROI analysis to compare differences in DTI parameter values between the patients and controls. A result with $p<.05$ was considered statistically significant. The statistical analysis was performed using GraphPad InStat software (GraphPad Software, San Diego, California).

The Randomise tool (FMRIB), a permutation program enabling modelling and inference (thresholding) using the standard general linear model design setup (Nichols and Holmes 2002), was used for two-regressor analysis (equivalent to an unpaired t-test) to perform voxelwise analysis of the FA, MD, AD, RD and volumetric analysis (Smith and Nichols 2009). Five thousand permutations of the data were generated to build up the null distribution. Age was used as a covariate for both voxelwise analysis of DTI parameters and volumetric analysis. Gender was also used as a covariate for voxelwise TBSS analyses.

5. RESULTS

5.1. MS in pregnancy (Studies I and II)

5.1.1. MS disease activity in pregnancy and post-partum (Studies I and II)

5.1.1.1. Clinical MS disease activity (Studies I and II)

The annualised relapse rate before, during and after pregnancy are shown in Figure 3. In Study I, the annualised relapse rate in the third trimester was significantly lower compared to the relapse rate during the year before pregnancy (p=0.04) and to the relapse rate 0-3 months post-partum (p=0.002). The relapse rate 0-3 months post-partum was higher than year before pregnancy (p=0.048). Of the 28 patients taking part in the study I, 68% were entirely relapse-free during pregnancy. During the 6-month post-partum follow-up, 15 of the 28 patients had experienced 19 relapses and the EDSS was slightly increased during the entire follow-up period of 35 weeks (0.95 ± 0.20 at 10-12 gestational weeks vs. 1.39 ± 0.22 6 months post-partum; mean ± standard error of mean [SEM]; p=0.048, paired Student´s t-test). In Study II with its lower number of study subjects (n=19), the alteration in EDSS during follow-up remained non-significant (1.24 ± 0.29 at 10-12 gestational weeks vs. 1.45 ± 0.28 6 months post-partum; mean ± standard error of mean; p=0.21, paired t-test).

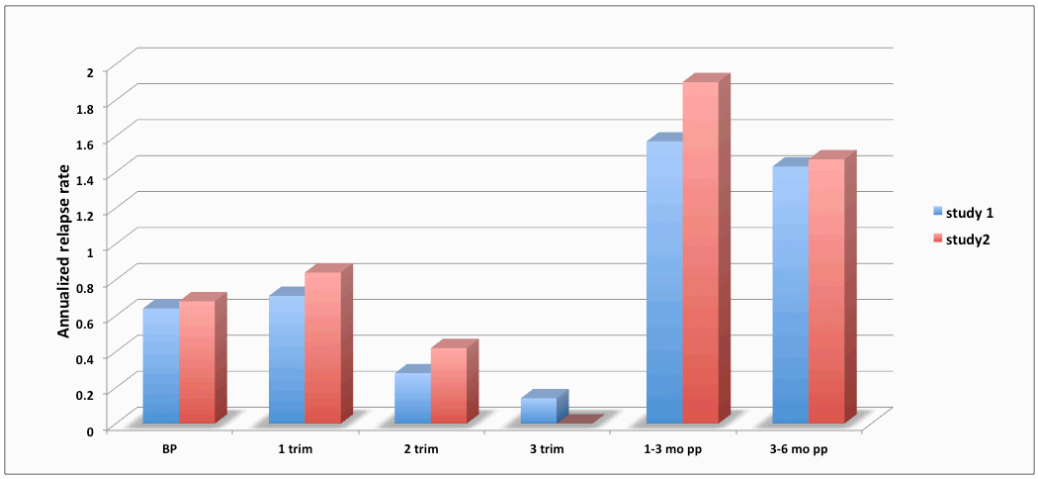

Figure 3. Annualised relapse rates before, during and after pregnancy in studies I (n=28) and II (n=19).

5.1.1.2. Number of MS lesions (Studies I and II)

The numbers of lesions in the MRI scans performed during the third trimester and post-partum are shown in Table 5. There was a significant increase in the hyperintense lesions in T2-weighted and DW images as well as in the total lesion load measured from FLAIR images in scans performed after the delivery when compared with the scans taken during pregnancy (Fig. 4). Lesions with diffusion restriction, i.e. having a lowered signal compared to NAWM on ADC maps, were not observed. No alteration was observed in the number of T1-lesions. Fourteen and eleven (50% in Study I; 58% in Study II respectively) of the patients showed radiological signs of MS activity (i.e. the scans contained one or more new, enlarging or Gd-enhancing lesions) in at least one of their post-partum scans.

Table 5. Numbers of lesions appearing hyperintense on T2-weighted images, hypointense ("black holes" and lesions darker than NAWM but brighter than CSF) on T1-weighted images and hyperintense on DW images on the first MRIs imaged in the third trimester and post-partum. Total volume of lesions appearing hyperintense on FLAIR-images. p-values are for Wilcoxon matched-pairs signed-rank test. SEM, standard error of mean.

	third trimester	post-partum	p-value
T2 LESIONS			
Study I (n=28)			
mean ± SEM	27.2 ± 5.5*	28.9 ± 5.6*	**0.002**
range	2-120	2-120	
median	13	15.5	
Study II (n=19)			
mean ± SEM	27.3 ± 7.2	29.2 ± 7.3*	**0.007**
range	5-120	4-120*	
median	12	13	
T1 LESIONS			
Study I (n=28)			
mean ± SEM	4.1 ± 0.9*	4.5 ± 1.0*	0.188
range	0-18	0-18	
median	3	3	
Study II (n=19)			
mean ± SEM	4.0 ± 1.0*	4.6 ± 1.2*	0.188
range	0-18*	0-18*	
median	3*	3	
DWI HYPERINTENSE LESIONS			
Study I (n=23)			
mean ± SEM	3.3 ± 0.5*	3.8 ± 0.6*	**0.016**
range	0-10*	0-12*	
median	3	4	
Study II (n=19)			
mean ± SEM	3.5 ± 0.6	4.1 ± 0.7	**0.024**
range	1-10	0-12	
median	3	4	
TOTAL LESION LOAD (ml)			
Study I (n=28)			
mean ± SEM	11.8 ± 3.2	12.8 ± 3.3	**0.027**
range	0.5-78.6	0.4-82.4	
median	6.16	6.96	
Study II (n=19)			
mean ± SEM	11.3 ± 2.8	12.3 ± 2.9	**0.029**
range	2.1-46.2	2.3-45.9	
median	6.65	7.44	

* Error in the original publication. The errors had no effect on the significance of the p-values.

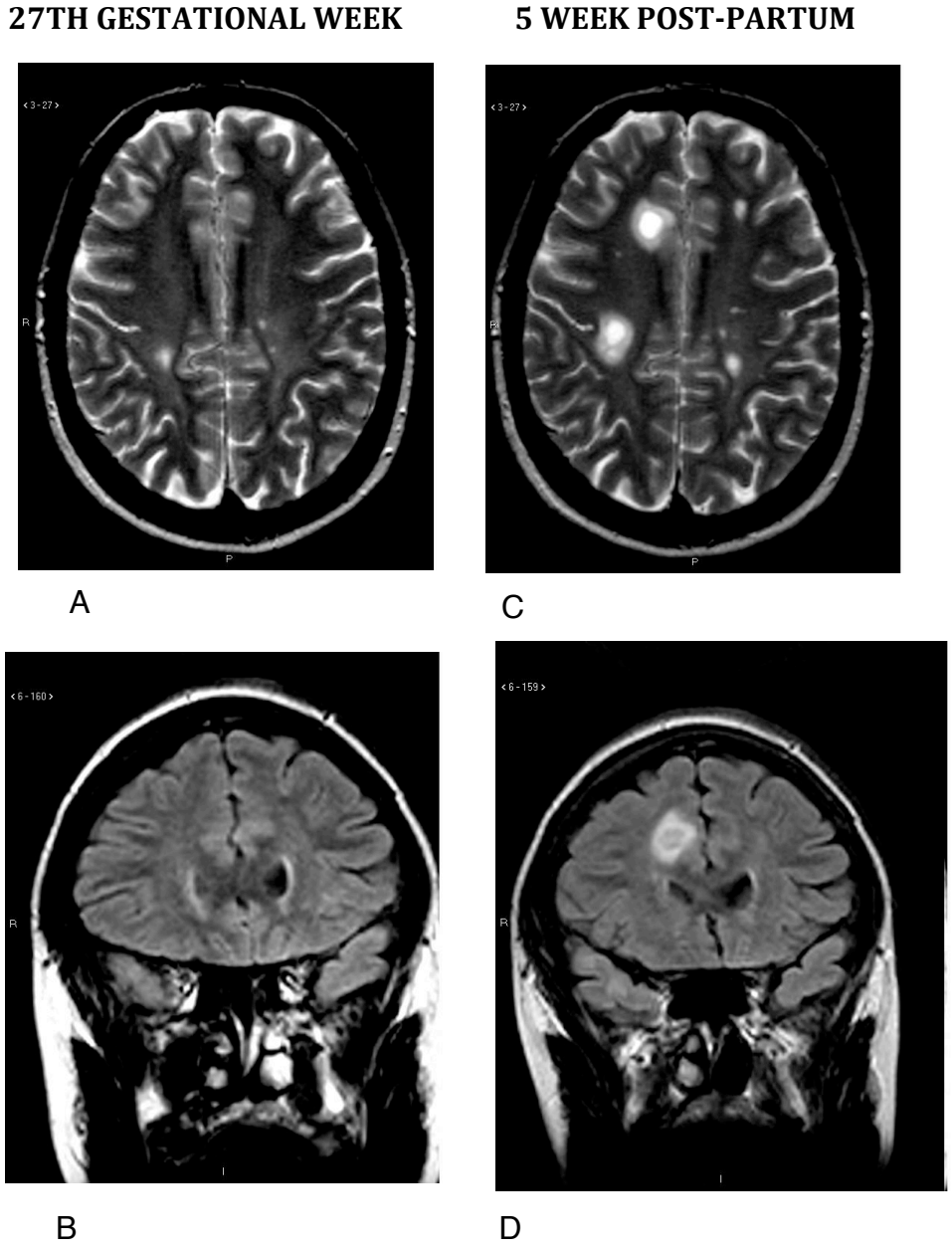

Figure 4. Patient with MS having small lesions in the centrum semiovale and periventricularly in the beginning of the third trimester in T2-weighted (A) and FLAIR-images (B). Corresponding images (C and D) obtained in the 5th post-partum week show two large lesions with surrounding oedema in the right centrum semiovale. One of these large lesions is new compared to the pre-partum image and the other has grown substantially. In the left centrum semiovale, one lesion has grown compared to the pre-partum image and there are also three new relatively small lesions.

5.1.1.3. Clinical vs. radiological activity (Study I)

Eight of the 14 patients (Study I) with active lesions in a post-partum scan experienced a clinical relapse during the follow-up period and 8 of the 14 patients with new or enlarging T2-lesions also had Gd-enhancing lesions. A total of 6 patients were scanned twice during the third trimester of pregnancy. Two of these 6 patients had T2-activity in the second pregnancy scan, as well as in the scan performed after the delivery. Another 2 of these 6 patients had T2-activity only in the post-partum-scan and 2 patients had no T2-activity in any of the scans. The numbers of new or growing lesions as a function of time in patients imaged more than once during, or after, pregnancy are illustrated in Figure 5. Six patients had early post-partum MRI activity but no clinical relapse within 6 months of delivery. On the other hand, 6 patients who did experience a relapse at 8-26 weeks post-partum showed no MRI activity in the scan performed 5-6 weeks post-partum, probably due to the delay between imaging and the time of relapse. During the post-partum period in total, 21 out of 28 (75%) patients demonstrated MS disease activity either by a clinical MS relapse or by T2-activity in the MRI scans.

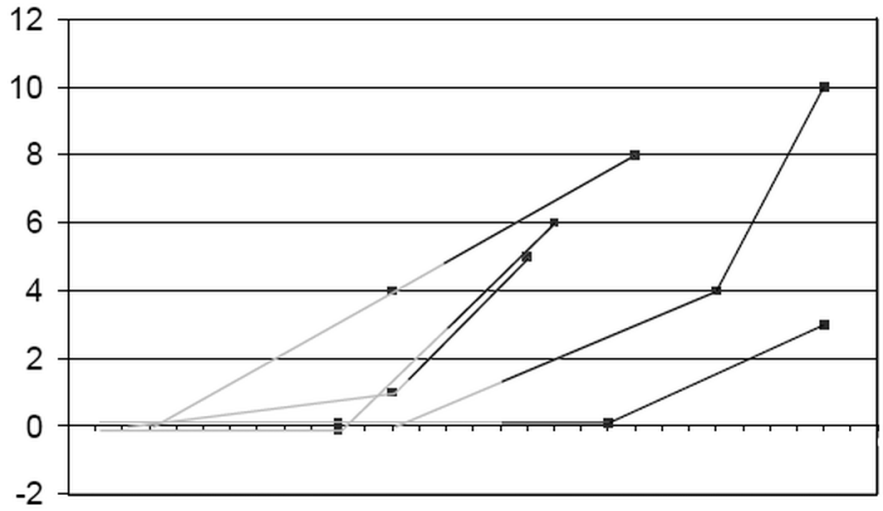

Figure 5. Demonstration of the number of active lesions (y-axis) as a function of time (x-axis, stacks at weekly intervals) in five patients. The number of active lesions on each MR scan is indicated by black dots. The time point at which each curve turns darker indicates the time of delivery. In all of these patients, active lesions are present at least in the last post-partum scan. The other four patients imaged more than twice showed no T2-activity on their scans.

5.1.2. Whole-brain ADC histograms in pregnancy and post-partum (Study II)

The average of the mean ADC-value was significantly lower in post-partum images than pre-partum images (p=0.026). The peak position of the ADC histogram was also significantly shifted to lower values in the post-partum images (p=0.014). The ADC data of patients scanned in the two imaging centres are detailed in Table 6. The averaged whole-brain ADC histograms of the patients imaged in Turku are shown in Figure 6.

Despite the overall lower ADC values in the post-partum setting, we observed higher mean ADC values in three patients (Fig. 7). The patient with the most prominent elevation in their mean ADC experienced a relapse severe enough to necessitate methylprednisolone pulse therapy at week six (deteriorated vision, clumsiness and dysesthesia in right hand, difficulties in walking). This took place shortly after the imaging. This patient also had the most prominent disease activation assessed by conventional MR scans, with 14 new T2 lesions and a 92% increase in lesion volume (6.4 ml pre-partum and 12.3 ml post-partum).

Table 6. Whole brain ADC histogram parameters of the patients imaged in the two different imaging centres. The ADC histogram parameter values are expressed in units of mm^2s^{-1} x 10^{-6}. ADC, apparent diffusion coefficient; SD, standard deviation.

	pre-partum	post-partum	p-value
TURKU (n=11)			
mean ± SD	781 ± 22	771 ± 23	**0.042**
peak position ± SD	766 ± 22	753 ± 24	**0.014**
HELSINKI (n=8)			
mean ± SD	896 ± 34	886 ± 36	0.313
peak position ± SD	889 ± 33	875 ± 34	0.313
ALL PATIENTS (n=19)			
mean			**0.026**
peak position			**0.014**

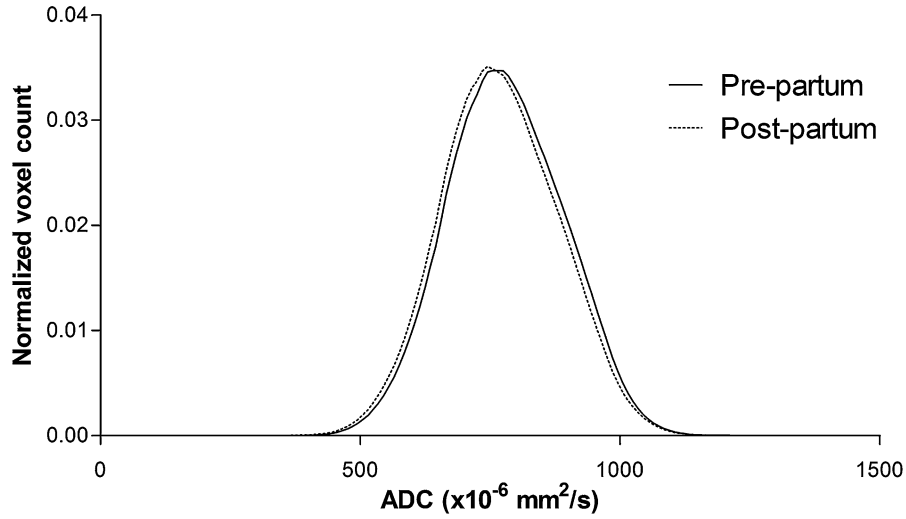

Figure 6. Mean ADC histogram of patients imaged in Turku showing a shift to lower ADC values after delivery (dotted line) compared with late pregnancy (solid line).

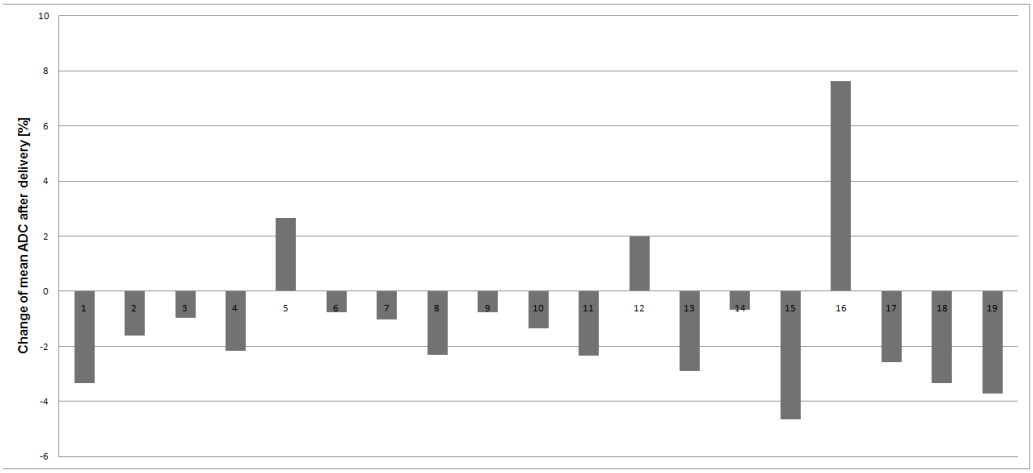

Figure 7. Bar graph showing percentual change of the mean ADC in each individual patient (1-19) after delivery. Only three patients had higher ADC values post-partum. Patient no. 16, having the most prominent rise in ADC, was the only patient who had significant clinical deterioration post-partum.

5.1.3. Brain volumetry in pregnant MS patients (Study II)

PBVC (mean -0.65, SD 1.1) showed a shift to larger brain volumes in 6 out of 19 patients and a shift to smaller volumes in 13 out of 19 patients. The ADC% did not exhibit correlation with the PBVC (r=- 0.18, p=0.46) or with VOL% (r=0.26, p=0.27).

5.2. MS patients with IFN-β treatment (Study III)

5.2.1. T2 lesion load (Study III)

At least one new T2 lesion was detected in the second MRI in 5 out of 9 nine patients. The same 5 patients had at least one Gd-enhancing lesion either in the first or second MRI. There was no significant change in the lesion volumes between the first and second MRI (p=0.57). The average lesion volume was 12.7 ml (SD 18.5 ml, range 0.9-60 ml) in the first MRI and 11.1 ml (SD 14.6 ml, range 0.3-48 ml) in the second MRI. The highest lesion load was 60 ml in the first MRI. The same patient also had the highest (48 ml) lesion load in the second MRI. In all other patients, the lesion load was less than 18 mls in both MRIs.

5.2.2. ADC histograms in the follow-up (Study III)

There was no statistically significant difference in ADC parameter values between the first and second imaging. Four of the five patients with new T2-lesions had a decrease (shift to lower values) in ADC histogram parameter values and one had an increase (shift to higher values). The ADC histograms of the patient with the increase as well as the histograms of one of the five patients with a decrease in ADC values are shown in Figure 8. The five patients with continuous disease activity had a significantly larger magnitude of change in histogram parameter values of the upper quartile (p=0.016) and mean (p=0.032) when compared to the four patients without new T2-lesions (Fig. 9). The difference in magnitude of change of median (p=0.19) and lower quartile (p=0.14) of the ADC histogram remained non-significant.

The number of new T2 lesions showed a positive correlation with the magnitude of change of the mean (r=0.79, p=0.014) and upper quartile (r=0.77, p=0.021) values of the ADC histogram, whereas the correlation between the number of new lesions and the magnitude of change of median (r=0.52, p=0.15) and lower quartile (r=0.46, p=0.21) values was not significant.

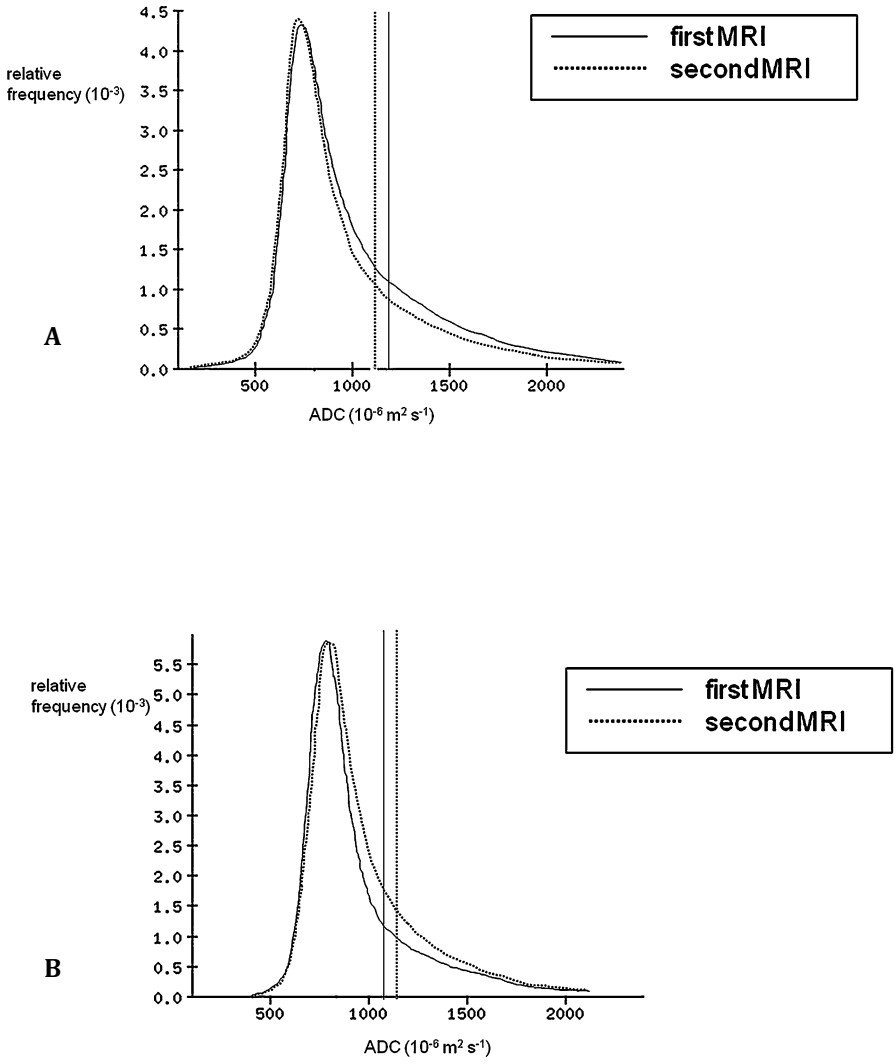

Figure 8. ADC histograms at the initiation of the study and at three-month follow-up in two patients with new T2 lesions. A shift either to lower (A) or higher (B) ADC-values on the second imaging is possible. The vertical lines represent the positions of the upper quartile of the histograms.

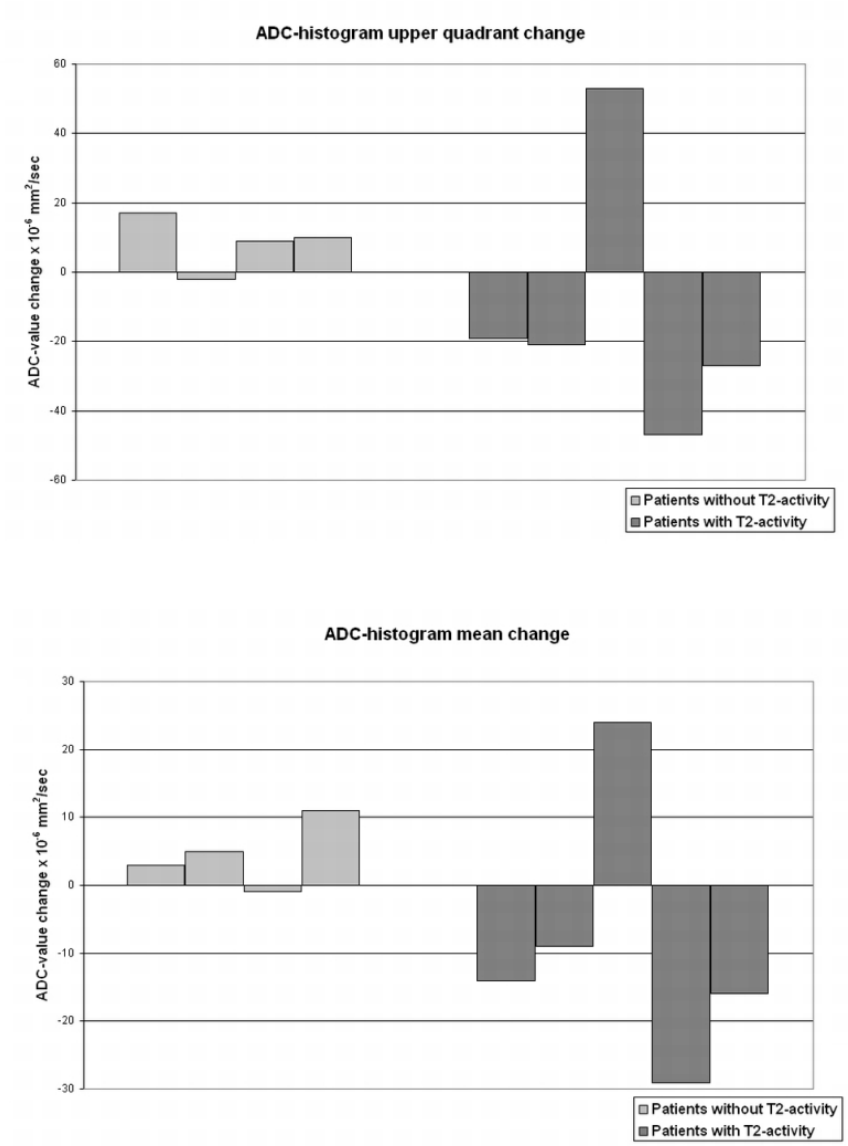

Figure 9. ADC histogram upper quartile (active vs. inactive, p=0.016) and mean (active vs. inactive, p=0.032) value change of four patients without and five patients with signs of disease activity on T2-weighted images three months after initiation of immunomodulatory treatment. Columns on the left: patients without new T2-lesions. Columns on the right: patients with new T2-lesions. ADC value is expressed in units of $10^{-6}mm^2/s$.

5.2.3. Brain volume analysis (Study III)

There was no significant difference in BVIs between the first and second MRI, and the difference in BVI between the first and second MRI was less than 0.5 percentage units in all patients. The change in BVIs did not correlate with the change in ADC values.

5.3. Fabry disease (Study IV)

5.3.1. White matter lesion load in FD (Study IV)

The mFs was 0 or 1 in 8 (67%) of the FD patients. Of those patients having a mild WML load, 5 had no T2-lesions and 3 had a mFs of 1. None of the study subjects having a mild WML load had lacunar or cortical infarctions visible on MR scans.

5.3.2. Voxelwise DTI analysis of FD patients (Study IV)

5.3.2.1. TBSS-analysis

With voxelwise TBSS analysis, we found widespread areas of decreased FA values in FD patients compared to healthy controls. Areas of reduced FA were found bilaterally in the pons along the corticospinal tract, the thalami, internal capsules, external capsules, corpus callosum and parietal white matter. Also, local areas of reduced FA were detected in the inferior longitudinal fasciculus and inferior fronto-occipital fasciculus and frontal white matter of the right side, and in the dorsal cingulum of the left side (Fig. 10). In voxelwise MD analysis, we found significantly increased MD values in both cerebellar hemispheres, the corona radiata and thalami and in the genu and splenium of the corpus callosum of the FD patients. Significant MD increases were also observed in the right frontal and parietal white matter and capsula interna of the FD patients (Fig. 11). We did not find any regional increases in the FA values or decreases in the MD values of FD patients compared to healthy controls.

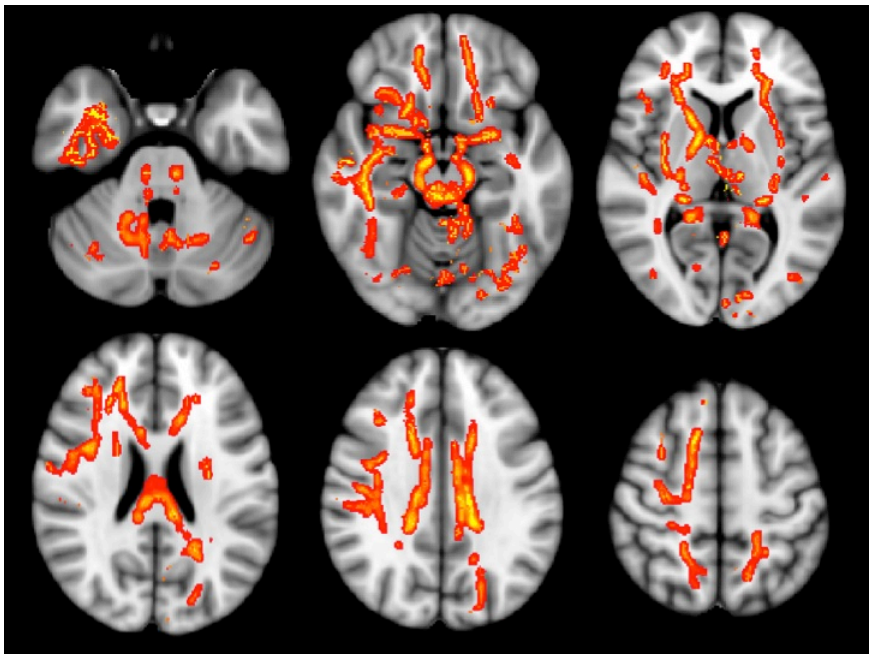

Figure 10. Statistically significant group difference of FA values lower in FD patients (n=12) compared to controls (n=13). Red-yellow scale represents p values 0.05-0.005. All p-values are family-wise error corrected for multiple comparisons. The significant findings are overlaid on a standard MNI152 image.

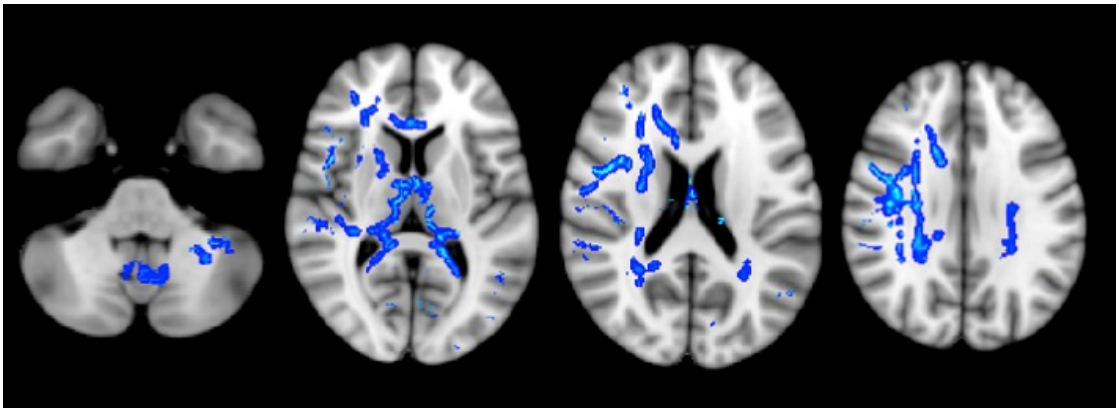

Figure 11. Statistically significant group difference of MD values higher in FD patients (n=12) compared to controls (n=13). Blue-light blue scale represents p-values 0.05-0.005. All p-values are family-wise error corrected for multiple comparisons. The significant findings are overlaid on a standard MNI152 image.

5.3.2.2. TBSS-guided ROI analysis

Patients with a severe burden of WMLs (i.e. a mFs of 2 or 3) were excluded from the ROI analysis. In the ROI analysis, which was guided by the TBSS findings, the 8 FD patients with mild WML load had significantly lower FA values compared to 8 healthy controls (Table 7). Also, significantly elevated RD values in FD patients were detected in this analysis. In contrast, no statistically significant MD differences were detected in the TBSS-guided ROI analysis.

The TBSS analysis between 8 FD patients and 8 controls did not reveal significant differences in FA, MD, AD or RD. Moreover, the TBSS analysis between patients with and without ERT revealed no significant differences in any of the four measured DTI parameters.

Table 7. Mean DTI parameter values and standard deviations of study subjects in TBSS-guided ROI analysis. FA, fractional anisotropy; MD, mean diffusivity; AD, axial diffusivity; RD, radial diffusivity.

FA (Mean±SD)	patients	0.492 ± 0.019
	controls	0.526 ± 0.014
	p	**0.0013**
MD (Mean±SD)	patients	642 ± 12
(x 10^{-6} mm^2/s)	controls	626 ± 15
	p	**0.037**
AD (Mean±SD)	patients	1019 ± 20
(x 10^{-6} mm^2/s)	controls	1030 ± 14
	p	0.240
RD (Mean±SD)	patients	471 ± 48
(x 10^{-6} mm^2/s)	controls	424 ± 17
	p	**0.020**

5.3.3. Brain volume analysis in FD (Study IV)

Normalised total brain tissue volume (patients 1488 ± 129 cm^3, controls 1501 ± 87.0 cm^3) and grey matter volume (patients 784 ± 118 cm^3, controls 765 ± 54.0 cm^3) did not significantly differ between FD patients and controls. FD patients had lower normalised white matter volumes (704 ± 30.0 cm^3) than normal controls (735 ± 45.9 cm^3), but the difference did not attain statistical significance ($p=0.057$).

The FSL-VBM analysis did not reveal regional differences in grey matter volumes between patients and controls.

6. DISCUSSION

In the present study, MRI and DWI of the brain have been used to follow changes occurring in the brain tissue of RRMS patients, comparing clinical and MR data before and after delivery and before and after initiation of DMT. The main focus was to investigate whether DWI can reveal changes that are not visible on conventional MR scans. Furthermore, we performed a voxelwise DTI study with FD patients to reveal possible microstructural alterations before excessive WML load is visible on conventional MR sequences.

6.1. DWI in pregnant MS patients

6.1.1. MS disease activity during pregnancy and post-partum (Studies I and II)

In Studies I and II, using MRI imaging, we have demonstrated that MS is activated soon after delivery, as the majority of the patients demonstrated new T2-lesions in images taken as soon as 4-5 weeks post-partum. There was also a statistically significant increase in DWI hyperintense lesions in the post-partum scans compared to images taken in the third trimester of pregnancy. During the 6-month post-partum follow-up period, disease activity was observed either in the form of a clinical relapse or as T2-activity in the MRI in 75% of the patients. The relapse rate was significantly reduced during the third trimester of pregnancy and increased post-partum. MRI seems to be a more sensitive method for assessing MS activity than recording relapses, because nearly half of the patients with early post-partum MRI activity experienced no symptoms or signs of clinical relapse during the follow-up period.

A few earlier prospective studies have addressed the relapse rate of MS during and after pregnancy. In the first two studies performed no change was observed in the relapse rate during pregnancy when compared to a self-control group (Sadovnick et al. 1994) or to a matched control group (Roullet et al. 1993). The PRIMS study (Confavreux et al. 1998), on the other hand, convincingly demonstrated that the risk of relapse in patients with MS declines significantly during the third trimester of pregnancy, only to increase three-fold in the first three months post-partum. The study of Finkelsztejn et al. (2011) showed a six-fold reduction in the relapse rate during pregnancy compared to the pre-pregnancy level and again a 3.5-fold increase in the 6 months after the delivery compared to the pregnancy level. Our study confirms the clinical results of the relapse rate alterations shown in the two latter studies: a transient, pregnancy-induced, remission and rebound in the post-partum period. According to Vukusic et al. (2004), factors associated with a higher risk of post-partum attacks in women with MS are a higher frequency of attacks prior to pregnancy, relapses during pregnancy and a higher level of physical disability prior to pregnancy. In our study cohort, no such correlations could be demonstrated (data not shown), presumably because of the smaller sample size.

There are no previous MRI studies of any larger MS cohort addressing disease activity during pregnancy or the post-partum period. A case study reported a decrease in the number of active lesions during the second half of pregnancy and a return of WML load to pre-pregnancy levels in the first months post-partum in two women with MS (van Walderveen et al. 1994). In addition, Saraste et al. described a patient with a very high number of Gd-enhancing lesions in a scan performed only four weeks after delivery (Saraste et al. 2006).

In Study I, for the majority of our patients (9/14), the post-partum scans demonstrating disease activity were performed within five weeks of delivery. This indicates that MS disease activation commonly takes place at a very early stage after delivery. Furthermore, we were surprised to observe the appearance of active lesions in two scans performed at 35-37 gestational weeks. This suggests that alterations might take place in the mothers' immune system during very late pregnancy as preparation for the delivery of the foetus. Interestingly, estriol concentration in the blood starts to decline after 35 gestational weeks, reflecting the dysfunction of the ageing placenta (Messiano and Jaffe 2004). Consequently, the loss of high estriol concentrations might lead to an increase in MS activity in certain patients.

It is well known that acute demyelinating lesions in patients with MS demonstrate increased ADC and hyperintensity in diffusion-weighted images (Castriota-Scanderbeg et al. 2002; Horsfield et al. 1998; Schaefer et al. 2000) that have been assumed to be due to vasogenic oedema. However, there are reports (Balashov et al. 2011; Gass et al. 2001) which have shown hyperacute demyelinating lesions with ADC values lower than the surrounding brain tissue consistent with cytotoxic oedema. In these two studies the lesions presenting initially with a low signal on ADC, when "pseudonormalised", and later showed increased diffusivity, consistent with turning towards vasogenic oedema in the follow-up MRI taken 5-10 days after the initial scan. In the report of Gass et al. (2001), the lesion which initially had diffusion restriction and later contained vasogenic oedema remained hyperintense in DW images obtained 5 weeks after the hyperacute phase, although less intense than on the initial scan. Hence, the hyperintensity of the acute (but not hyperacute) lesion is due to "T2 shine-through". Indeed, in these two previous reports (Balashov et al. 2011; Gass et al. 2001), the T2 intensity of the acute phase lesions became higher compared to the hyperacute phase, keeping the lesions hyperintense on DW images even though the ADC of the lesions was rising.

In our study I, there was a statistically significant increase in DWI hyperintense lesions in post-partum scans compared with MRIs taken during the third trimester. These lesions were not hypointense on the ADC maps. Hence, the high signal in DWI images was due to "T2 shine-through", not due to cytotoxic oedema. Not all of the DWI-hyperintense lesions in the post-partum scans were necessarily acute lesions, but we believe that our finding of a significant increase in the number of DWI-positive lesions partly reflects the early activation of MS after delivery, i.e. the new DWI-hyperintense lesions may have been acute lesions in their "pseudonormal" (beginning of vasogenic oedema) phase. The statistically significant increase of T2-lesions on post partum scans supports this interpretation.

Given the almost universal tendency for disease activation in the post-partum period, we see no need for routine MRI scanning of MS patients during pregnancy or the post-partum period. Treatment decisions can, mostly, be made on clinical grounds, while MRI imaging can be applied in more problematic cases. Our finding of early new post-partum lesions in brain MRI has implications for the treatment of mothers with MS. To prevent post-partum relapses, disease-modifying treatment should be initiated as early as possible.

6.1.2. Whole-brain diffusity in MS patients during pregnancy and post-partum (Study II)

In Study II we used the same patient data and MRI scans as in Study I, excluding the 5 patients imaged in Tampere (no DW images) and 4 patients imaged in Helsinki (image quality not sufficient for generating histograms). Surprisingly, we found a slight but statistically significant decrease of whole brain ADC in images obtained 4-12 weeks after delivery, even though the WML load was also significantly higher post partum compared to the third trimester of pregnancy in this patient cohort. The higher ADC values observed during the pregnancy of the MS patients are likely to be due to the physiological changes taking place in the cerebral vasculature during pregnancy, which overcome the inflammation-induced effects on ADC. Hence, our study confirms that ADC histogram analysis is of limited value in the follow-up of inflammatory conditions in a pregnancy-related setting.

Normal pregnancy is associated with significant haemodynamic and cardiovascular changes in order to meet the metabolic needs of the mother and the foetus: the maternal cardiac output and plasma volume increase during pregnancy, while the total vascular resistance and blood pressure tend to decrease (Khalil et al. 1998). In an MR study using velocity-encoded phase contrast sequences with 10 healthy pregnant volunteers, a significant reduction in brain blood flow was detected in late pregnancy. This finding was thought to represent generalised vasodilatation of downstream resistance arterioles, assuming constant blood flow at the tissue level (Zeeman et al. 2003).

The pregnancy-related alterations in cerebral vasculature may contribute to the oedema and neurological defects seen with preeclampsia-associated hypertension. It has been postulated that the pathophysiology of eclampsia includes increased permeability of small vessels due to endothelial injury, and hypertension-induced breakdown of cerebrovascular autoregulation. These factors may cause brain lesions with vasogenic oedema. If the vasogenic oedema progresses, it may result in an increase in local tissue pressure, a decrease in regional perfusion pressure and a reduction of blood flow to irreversible ischemic levels with cytotoxic oedema. Regarding eclamptic encephalopathy, diffusion-weighted imaging has proved to be a valuable tool in differentiating between vasogenic and cytotoxic oedema in brain lesions, the former having elevated ADC values and the latter having decreased ADC values (Engelter et al. 2000; Koch et al. 2001; Schaefer et al. 1997; Ulrich et al. 2006; Watanabe et al. 2002). Our finding of slightly but statistically significantly higher ADC during the third trimester in relation to post-partum imaging is likely to reflect the physiological state of late pregnancy, representing a possible predisposing factor to pregnancy-related

hypertensive encephalopathy.

Increased brain ADC has been reported both in MS lesions and in NAWM during MS disease activity (Droogan et al. 1999; Garaci et al. 2007). Decreased FA in the normal-appearing corpus callosum, reflecting occult injury of white matter tracts in MS patients has also been reported (Lou et al. 2009). MS lesions are heterogenous in terms of their ADC values. Relatively low ADC values have been found in homogeneously enhancing lesions and at the border of ring-enhancing lesions (Filippi et al. 2000; Roychowdhury et al. 2000), but these lesions are still reported to have higher ADC than the NAWM has (Roychowdhury et al. 2000). However, diffusion restriction has also been reported in hyperacute lesions, as mentioned above. In our study, no lesions with hypointensity were detected on ADC maps. The numbers of MS lesions in our patients either increased or remained the same after delivery and the overall lesion load of the patients was relatively small. At the same time, the ADC values tended to decrease. Therefore, we believe that our finding of decreasing ADC after delivery is not due to the change in the number of MS lesions. In summary, we believe that our finding of decreasing ADC after delivery is due to physiological changes within the NAWM. Masking the lesions out from the histograms might have strengthened but not changed our finding. However, in this kind of longitudinal study, there would be several possible sources of error in lesion segmentation, e.g. a selection bias at the voxel level between the two time points.

Interestingly, the patient who had the worst post-partum relapse (including a 1.5 point increase in EDSS) had a nearly 8% increase in their mean ADC. It seems that in this case the prominent post-partum disease activity induced a strong enough increase in the ADC value to exceed the physiological post-partum related reduction in ADC. The increase in the post-partum lesion volume probably had some influence on the histograms, but since the absolute increase in the lesion volume was still relatively small (5.9 ml), we believe the major factor leading to increased post-partum ADC was MS related alterations in the NAWM. This is in line with a previous longitudinal study reporting a correlation between ADC and clinical disability (Garaci et al. 2007).

Corticosteroid therapy has been proved to decrease brain ADC both in patients with brain pathology and in patients without brain pathology receiving corticosteroid therapy for other indications (Minamikawa et al. 2004). Our patients did not receive corticosteroid therapy during pregnancy or after delivery before their follow-up MR scans. Moreover, no DMT was initiated during the follow-up period. This permits us to conclude that the ADC changes detected are not attributable to medication.

6.2. Diffusion weighted imaging in multiple sclerosis patients having IFN-β treatment (Study III)

In Study III we studied 9 patients with active newly diagnosed MS with two to three relapses during the year preceding the first MRI. IFN-β treatment was initiated soon after obtaining the first imaging. The five patients having at least one new and enhancing lesion in the conventional images of their second scan had more prominent changes in ADC values than the patients without signs of disease activity. Four of the

patients with signs of disease activity had a shift to lower ADC values and one to higher values on their second scan.

Our finding is somewhat counterintuitive in the light of earlier study reports. There are a few earlier longitudinal studies on patients with active MS, but most of the patients in these studies are not on treatment for MS. In ROI based longitudinal analyses on patients with active MS, a significant increase of ADC has been seen in NAWM areas in which Gd enhancing lesions subsequently developed (Rocca et al. 2000; Werring et al. 2000). In the same study by Werring et al., a milder, but statistically significant increase in ADC was also seen in anatomically matched contralateral regions (which appeared normal in the conventional images during the whole follow-up period) at the time point of the first noted lesion enhancement. In another longitudinal study based on histogram analysis of non-treated patients with active MS, a significant increase of MD was detected in NAGM, but not in NAWM (Oreja-Guevara et al. 2005). In a longitudinal study, an increase in MD of NAGM and NAWM was also shown to predict later clinical progression of MS (Rovaris et al. 2006).

In a recent longitudinal study, 44 patients having MS were analysed twice (baseline and follow-up at a median of 12 months) with DWI (Sämann et al. 2012). To our knowledge, the Sämann study is the only one, in addition to ours, in which the majority (37 out of 44) of patients were on DMT. The main finding in Sämann´s study was that higher baseline mean ADC predicts later clinical progression of MS. They also found a slight but statistically significant elevation of mean ADC in the follow-up. However, the mean annualised ADC elevation was only 4 x 10^{-6} mm^2/s with standard deviation of 13 x 10^{-6} mm^2/s, which means that they met with both increases and decreases of mean ADC in the follow-up MRI. In addition, both increases and decreases of mean ADC were observed in our study. In fact, there was a slight shift to lower values in the average of the mean ADC of the MS patients in our study, albeit this shift was not statistically significant.

It has been postulated that subtle BBB damage also occurs in areas of MS patients' white matter located far from the lesions that are visible on conventional images (Vrenken et al. 2006). It has also been shown that IFN-β reduces the permeability of BBB in vitro (Müller et al. 2012; Niemelä et al. 2008). Therefore, it is possible that our findings of mean ADC shifts to a lower level may be at least partly caused by DMT-induced stabilisation of BBB. This resolution of the disease-related abnormal permeability of BBB caused by DMT has also been postulated to cause the pseudoatrophy seen in the first months after the initiation of DMT. In our study there was no reduction in the BVIs in MRIs obtained 3-4 months after the initiation of the IFN-β treatment and no correlation between percentual changes in BVI and ADC values.

Very solid conclusions cannot be made on the basis of our study with small group of patients and short follow-up time. Ideally, the influence of IFN-β treatment on the brain diffusivity of patients with newly diagnosed MS should be investigated by using several MR studies with short intervals. Furthermore, it would be highly interesting to correlate the changes of brain volumes and brain diffusivity in the first months of DMT. Probably this would give more information to clarify the mechanisms behind the

DMT-induced pseudoatrophy in the early phases of treatment.

6.3. DTI in FD (Study IV)

Study IV aimed to reveal possible disturbances in white matter integrity in the form of FA reduction in FD patients compared to healthy controls. Our study revealed widespread abnormalities of diffusion tensor parameters in FD patients. For the first time, we were able to reveal areas of FA reduction along with MD elevation. This finding suggests microstructural damage leading to loss of myelin integrity resulting in decreased anisotropic water diffusion in FD patients' brain white matter. This finding was also present in the ROI analysis for patients and controls with no WMLs or a mild burden of WMLs having exactly the same distribution of mFs (5 with an mFs of 0 and 3 with an mFs of 1). Our finding suggests that the FA reduction and MD elevation of FD patients´ white matter is already taking place in areas which appear normal on conventional MR scans, even though the separate TBSS analysis for these subjects with a mild WML burden did not reveal areas of significant difference in the DTI parameters in this small sample. It is possible that the statistical power of the TBSS analysis was not sufficient with this sample size to show the difference between the FD patients and the controls.

Our finding of reduced FA and among FD patients is non-specific. A previous autopsy case report concerning a patient with dementia associated with FD (Okeda and Nisihara 2008) revealed diffuse axonopathic leukoencephalopathy owing to multisegmental hydropic swelling of axons in the bilateral cerebral deep white matter. This reported histological oedematous axonopathy might be a reason for the weakening of the directional organisation of brain white matter detectable by DTI. On the other hand, in our study, the changes in FA values were because of elevated RD, according to the ROI analysis. Increased RD has been suggested to be a sign of myelin damage rather than an indication of axonal injury (Song et al. 2002). However, there are several possible pitfalls when interpreting changes in axial and radial diffusivities on the basis of the underlying tissue structure (Wheeler-Kingshott and Cercignani 2009). Hence, the exact neuropathological process behind our finding remains unknown.

Earlier studies have shown structural and metabolic brain abnormalities in patients without a significant WML load using DTI (Fellgiebel et al. 2006a; Albrecht et al. 2007), magnetic resonance spectroscopy (Tedeschi et al. 1999) and 18-fluoro-deoxyglucose PET (Moore et al. 2003). In an earlier study, significant increases in cerebral white matter MD in FD patients were found without significant WMLs (Albrecht et al. 2007). In contrast to our findings, they did not find areas of reduced FA in FD patients. There are some differences in the acquisition parameters between these two studies. For example, the DTI sequence was imaged with gradients along 6 non-collinear directions in Albrecht's study, whereas in our study, 16 gradient-encoding directions were used. However, the difference between the findings is more likely to be explained by the difference between the methods of statistical analysis. It has been demonstrated that the TBSS method may have higher sensitivity to FA changes compared with other methods using voxel based analyses (Smith et al. 2006; Focke et al. 2008).

We did not find significant differences in FA and MD between patients with and without ERT. However, no conclusions can be made on the effect of ERT based on this finding. This is because the patients with ERT, having a mean age 21 years higher than the patients without ERT, had been affected by FD for a substantially longer time than the non-treated patient group.

6.4. Limitations of the study

Studies I and II lack the reference group and therefore it is difficult to estimate how much of the observed increase in post-partum lesion load is attributed to the post-partum condition and how much to the natural course of MS. Another limitation of Studies I and II is that MRI were performed in three different centres, which might introduce an inter-centre variability in the MR image quality. However, the image post-processing and evaluation was centralised at a single imaging centre.

In Study II, separating the white and grey matter and focusing on the white matter only would have probably disclosed the finding more strongly. Unfortunately, the contrast between grey and white matter in our images was not sufficient enough for segmentation of white and grey matter.

In Study III, the weaknesses are the small number of patients and the lack of exact knowledge of the temporal development of the disease activity. As only two sequential MRI studies were carried out, it is difficult to determine the exact evolution (or cessation) of the inflammatory activity. Therefore, based on our material we cannot exactly determine the temporal relationship between the histogram changes and the signs of inflammatory disease activity.

In Study IV, we collected the DTI data with 1 mm intersection gaps between the slices, which is probably not optimal for the analysis of DTI data. MRI data is often acquired with a gap between slices in order to avoid crosstalk artefacts, which are introduced into images by interference between adjacent slices of a scan, caused by a slice profile that is not ideal due to the constraints of the measurement technology. In retrospect, it was probably unnecessary to have a gap between slices, because slices were acquired in interleaved order and the TR time in the acquisition was rather long (5451-5616 ms). However, we believe that it is highly unlikely that the intersection gap could induce a false positive finding of FA reduction, since the same DTI acquisition parameters were used for both the patient and control groups.

6.5. Future considerations

We found increased post-partum MD values with histogram analysis among mothers with RRMS when compared to pre-partum levels despite a significant increase in white matter lesions after delivery. We believe that our finding is due to physiological changes within the NAWM. Future DTI studies with healthy pregnant individuals performed with ROI-based and/or voxelwise analysis could provide regional information about MD increases. If the MD elevation is found to concentrate in the posterior brain territories, it could strengthen our assumption that the physiological state of late pregnancy could be a predisposing factor to pregnancy-related hypertensive encephalopathy. Even though the ADC histogram analysis seems to be of limited value in the follow-up of inflammatory conditions in a pregnancy-related setting, it is possible that measuring FA histograms could have more to offer in the follow-up of pregnant MS patients. Following the dynamics of brain FA with measures of healthy subjects before, during and after pregnancy could also offer more information on the changes occurring in the brain caused by pregnancy-related physiological mechanisms.

The histogram measures of DWI- or DTI-derived images could be clinically useful in the follow-up of the treatment effect of disease modifying drug in MS. Ideally, the association between different phases of relapse and DTI parameters should be investigated by using a number of short interval MR scans and including TBSS to follow white matter integrity voxelwise between different time points. Studies with larger patient group and with a control group are needed to clarify the effects of disease modifying drugs on NAWM in MS.

In Study I, 6 patients (21%) showed early post-partum MRI activity but no clinical relapse within 6 months of delivery. In Study III, 5 patients (56%) showed signs of disease activity in MRI scans obtained 3 to 4 months after the initiation of IFN-β treatment. In the future, as new effective therapies, which may be more expensive or may have more dangerous side effects than older therapies, become available, there might be a need for routine MRI control to detect sub-optimal responses to on-going therapy.

Our study revealed microstructural damage in the white matter of FD patients before excessive WML load was visible on conventional scans. It would be highly valuable to longitudinally monitor the natural course of FD and possible effect of ERT using voxelwise brain DTI analysis. Furthermore, it would be highly interesting to use this same method with other lysosomal storage disorders.

MRI studies with higher field strength could provide new views on the dynamics of cortical pathology in MS and improve the sensitivity of DTI to reveal even more pathologies not visible in conventional MRI scans or DTI performed with lower MR field strength in FD.

7. CONCLUSIONS

Based on the results of this thesis at 1.5 T, we conclude the following:

I Increased amounts of T2-hyperintense and DWI-hyperintense lesions were shown as early as 4 to 7 weeks after delivery as a sign of the early clinical post-partum activation of MS. Post-partum activation is an early and common phenomenon amongst mothers with MS. It is important to initiate DMT as early as possible to prevent post-partum relapses. MRI seems to be a more sensitive method for assessing MS disease activity than recording relapses.

II Longitudinal evaluation with ADC histogram analyses of pregnant MS patients and MS patients with DMT shows controversial results which are affected by changes in disease activity and the physiology of mothers with MS soon after delivery. Whole brain ADC is not a reliable measure in determining the disease activity of MS in pregnant patients.

III RRMS patients with signs of disease activity may show shifts to either lower or higher global brain tissue ADC values. Further studies are needed to investigate which factors in the RRMS patients´ brain tissue correspond to the alterations in ADC values. It is probable that the disease progression pulls the ADC values to higher values and disease-modifying treatment pulls them to lower values.

IV MD and FA measured with DTI can show microstructural damage in the brain white matter of FD patients before excessive white matter changes are visible on conventional MR scans. FA and MD could be a valuable tool in monitoring the possible effects of treatment options in FD.

8. ACKNOWLEDGEMENTS

This study was carried out at the department of Radiology, University of Turku, during the years 2005–2012. It was financially supported by grants from Turku University Hospital (EVO grants).

I wish to express my sincere gratitude to the following people:

Professor Hannu Aronen, for his encouragement, practical advice and inspiring enthusiasm for science.

Professor Riitta Parkkola, thesis supervisor, for her enormous knowledge, pragmatism and never-ending energy as well as for her positivity and for "kicking" at the right moments. Docent Laura Airas, thesis supervisor, for her vast knowledge of MS, her enthusiasm and professionalism in academic writing and also for her clinical examination of the MS patients in this study. Docent Timo Kurki, thesis supervisor, for his creativity and tremendous expertise in MRI imaging, as well as for organising the start of this study. I have been very lucky to have Riitta, Laura and Timo as my supervisors: they are not only brilliant researchers, but are also wonderful persons to collaborate with. Without them, it would not have been possible to accomplish this thesis.

Docent Auli Verkkoniemi-Ahola and Docent Tapani Tikkakoski, the official reviewers of this thesis, for their constructive comments and valuable feedback, which led to a marked improvement in the final form of this manuscript.

Professor Irina Elovaara and Professor Markus Färkkilä at Tampere University Hospital and Helsinki University Hospital respectively, for their clinical examinations of the pregnant MS patients in this study. Docent Oili Salonen and Docent Prasun Dastidar at Helsinki University Hospital and Tampere University Hospital respectively, for organising the MRI examinations of the pregnant MS patients in this study. Professor Ilkka Kantola, for his clinical examinations of the FD patients in this study. Professor Pirjo Nuutila and Professor Juhani Knuuti, head of the Turku PET Centre, for providing time and facilities for the MRI imaging of the FD patients. Kati Korhonen, MD, for her friendly collaboration.

The former and present head radiologists at the Medical Imaging Centre of Southwest Finland, Docent Anu Alanen, Juha Sjövall, MD, and Sakari Salo, MD for their favourable attidute towards research projects and for providing facilities for clinical work and research. Docent Kimmo Mattila, for his tireless encouragement and valuable advice regarding science projects and for taking part in the project's guidance group.

The brilliant pair of physicists, Virva Saunavaara MSc and Jani Saunavaara PhD, for their invaluable help in the tortuous problems into which I often fell in the fields of physics and IT. Docent Ronald Borra, Mikko Kankaanpää, PhD, and Markku Komu, MSc, for giving valuable advice and technical guidance in the early years of this study.

All of the radiographers who participated in this study for their seamless and accurate cooperation.

Mrs Pirjo Helanko and Mrs Jaana Keihäs for their flexible assistance in several bureaucratic issues, which were often complicated due to my last-minute changes to the original schedules.

All of the MS and FD patients who have participated in this study.

My colleagues at VSKK, especially all my current and former colleagues at A-Röntgen, for the inspiring and often hilarious atmosphere. Thank you for enduring my wooden jokes and tautological anecdotes. Thanks to you, an innumerable amount of good jokes have also been heard in venues like Cantina Tollo.

My fellow neuroradiologists, Pirkko Sonninen, MD, Jari Karhu, MD and Mikko Nyman, MD, for their endurance and for doing all the clinical work while I have been on leave because of my research projects.

My colleagues and co-partners at Irad Oy: Tomi Pudas, MD, Sami Virtanen, MD, Jussi Kankare, MD, PhD, Juha Ratilainen, MD, Ariel Koskinen, MD, Docent Erkki Svedström, Sami Kajander, PhD, and Tomi Teirmaa, MD. It is an honour for me to be a part of this team. It has not been only a great place to practice, but has also offered several refreshing and fruitful seminars on truly important themes. Hopefully we also have many of those ahead of us, because I still need lots of training, for example in oenology.

My friends for their patience since even the 70s. The tautology of my stories sometimes keeps on going even outside my workplaces. Thanks to Jouni, Miika and Kim for the sporty trips we have taken in recent years. I am looking forward for our future trips with long and outstandingly sophisticated discussions. The slices of Oak Barrel were…

My parents, Anja and Pekka Paavilainen, grandmother Eeva Fors, grandfather Elmer Fors, grandmother Sanna Paavilainen, "big sisters" Heli Kaunisto and Tiina Fors, and "big brother" Ari-Pekka Fors, for giving my life a solid and safe foundation.

My father-in-law, Sakari Kumlander, for help in numerous different issues ranging from babysitting to being a control subject in an MRI research project.

My wife, Teija and my daughters, Venla and Anni. Your love is the light of my life and has been the greatest help for me to win through the most difficult times.

Turku, May 2013

Teemu Paavilainen

9. REFERENCES

Afzali M, Soltanian-Zadeh H, Elisevich KV. Tract based spatial statistical analysis and voxel based morphometry of diffusion indices in temporal lobe epilepsy. Comput Biol Med 2011;41:1082-1091.

Albrecht J, Dellani PR, Müller MJ, Schermuly I, Beck M, Stoeter P, Gerhard A, Fellgiebel A. Voxel based analyses of diffusion tensor imaging in Fabry disease. J Neurol Neurosurg Psychiatry 2007;78:964-969.

Alexander AL, Lee JE, Lazar M, Field AS. Diffusion tensor imaging of the brain. Neurother 2007;4:316-329.

Anderson VM, Fox NC, Miller DH. Magnetic resonance imaging measures of brain atrophy in multiple sclerosis. J Magn Reson Imaging 2006;23:605-618.

Anderson W. A case of angiokeratoma. Br J Dermatol 1898; 10: 113–7.

Andersson JL, Jenkinson M, Smith S. Non-linear optimization. FMRIB Analysis Group Technical Report. TR07JA1. 2007a. www.fmrib.ox.ac.uk/analysis/techrep.

Andersson JL, Jenkinson M, Smith S. Non-rigid registration, aka spatial normalisation. FMRIB Analysis Group Technical Report. TR07JA2. 2007b. www.fmrib.ox.ac.uk/analysis/techrep.

Andréll P, Jensen C, Norrsell H, Ekre O, Ekholm S, Norrsell U, Eliasson T, Mannheimer C, Blomstrand C. White matter disease in magnetic resonance imaging predicts cerebral complications after coronary artery bypass grafting. Ann Thorac Surg 2005;79:74-80.

Ascherio A, Munger KL. Environmental risk factors for multiple sclerosis. Part I: The role of infection. Ann Neurol 2007;61:288-299.

Ashburner J, Friston KJ. Voxel-based morphometry - the methods. Neuroimage 2000;11:805-821.

Audoin B, Ibarrola D, Malikova I, Soulier E, Confort-Gouny S, Duong MV, Reuter F, Viout P, Ali-Chérif A, Cozzone PJ, Pelletier J, Ranjeva JP. Onset and underpinnings of white matter atrophy at the very early stage of multiple sclerosis–a two-year longitudinal MRI/MRSI study of corpus callosum. Mult Scler 2007;13:41-51.

Baker PN, Johnson IR, Harvey PR, Gowland PA, Mansfield P. A three-year follow-up of children imaged in utero with echo-planar magnetic resonance. Am J Obstet Gynecol 1994;170:32-33.

Balashov KE, Aung LL, Dhib-Jalbut S, Keller IA. Acute multiple sclerosis lesion: conversion of restricted diffusion due to vasogenic edema. J Neuroimaging 2011;21:202-204.

Banikazemi M, Bultas J, Waldek S, Wilcox WR, Whitley CB, McDonald M, Finkel R, Packman S, Bichet DG, Warnock DG, Desnick RJ; Fabry Disease Clinical Trial Study Group. Agalsidase-beta therapy for advanced Fabry disease: a randomized trial. Ann Intern Med 2007;146:77-86.

Barkhof F. The clinico-radiological paradox in multiple sclerosis revisited. Curr Opin Neurol 2002;15:239-245.

Barkhof F, Hommes OR, Scheltens P, Valk J. Quantitative MRI changes in gadolinium-DTPA enhancement after high-dose intravenous methylprednisolone in multiple sclerosis. Neurology 1991;41:1219-1222.

Bartha AI, Yap KR, Miller SP, Jeremy RJ, Nishimoto M, Vigneron DB, Barkovich AJ, Ferriero DM. The normal neonatal brain: MR imaging, diffusion tensor imaging, and 3D MR spectroscopy in healthy term neonates. AJNR Am J Neuroradiol 2007;28:1015-1021.

Basser PJ, Mattiello J, Le Bihan D. MR diffusion tensor spectroscopy and imaging. Biophys J 1994;66:259-267.

Battaglini M, Giorgio A, Stromillo ML, Bartolozzi ML, Guidi L, Federico A, De Stefano N. Voxel-wise assessment of progression of regional brain atrophy in relapsing-remitting multiple sclerosis. J Neurol Sci 2009;282:55-60.

Beaulieu C. The basis of anisotropic water diffusion in the nervous system - a technical review. NMR Biomed 2002;15:435-455.

Bendfeldt K, Blumhagen JO, Egger H, Loetscher P, Denier N, Kuster P, Traud S, Mueller-Lenke N, Naegelin Y, Gass A, Hirsch J, Kappos L, Nichols TE, Radü EW, Borgwardt SJ. Spatiotemporal distribution pattern of white matter lesion volumes and their association with regional grey matter volume reductions in relapsing-remitting multiple sclerosis. Hum Brain Mapp 2010;31:1542-1555.

Bermel RA, Bakshi R. The measurement and clinical relevance of brain atrophy in multiple sclerosis. Lancet Neurol 2006;5:158-170.

Bester M, Heesen C, Schippling S, Martin R, Ding XQ, Holst B, Fiehler J. Early anisotropy changes in the corpus callosum of patients with optic neuritis. Neuroradiology 2008;50:549-557.

Bloomgren G, Richman S, Hotermans C, Subramanyam M, Goelz S, Natarajan A, Lee S, Plavina T, Scanlon JV, Sandrock A, Bozic C. Risk of natalizumab-associated progressive multifocal leukoencephalopathy. N Engl J Med 2012;366:1870-1880.

Borden EC, Sen GC, Uze G, Silverman RH, Ransohoff RM, Foster GR, Stark GR. Interferons at age 50: past,

current and future impact on biomedicine. Nat Rev Drug Discov 2007;6:975-990.

Brabec J, Rulseh A, Horinek D, Pala A, Guerreiro H, Buskova J, Petrovicky P, Nemcova V, Krasensky J, Seidl Z, Nimsky C, Sonka K. Volume of the amygdala is reduced in patients with narcolepsy - a structural MRI study. Neuro Endocrinol Lett 2011;32:652-656.

Brex PA, Jenkins R, Fox NC, Crum WR, O'Riordan JI, Plant GT, Miller DH. Detection of ventricular enlargement in patients at the earliest clinical stage of MS. Neurology 2000;54:1689-1691.

Brusaferri F, Candelise L. Steroids for multiple sclerosis and optic neuritis: a meta-analysis of randomized controlled clinical trials. J Neurol 2000;247:435-442.

Burlina AP, Manara R, Caillaud C, Laissy JP, Severino M, Klein I, Burlina A, Lidove O. The pulvinar sign: frequency and clinical correlations in Fabry disease. J Neurol 2008;255:738-744.

Castriota-Scanderbeg A, Sabatini U, Fasano F, Floris R, Fraracci L, Di Mario M, Nocentini U, Caltagirone C. Diffusion of water in large demyelinating lesions: a follow-up study. Neuroradiology 2002;44:764-767.

Catalaa I, Grossman RI, Kolson DL, Udupa JK, Nyul LG, Wei LG, Zhang X, Polansky M, Mannon LJ, McGowan JC. Multiple sclerosis: magnetization transfer histogram analysis of segmented normal-appearing white matter. Radiology 2000;216:351-355.

Cercignani M, Inglese M, Pagani E, Comi G, Filippi M. Mean diffusivity and fractional anisotropy histograms of patients with multiple sclerosis. AJNR Am J Neuroradiol 2001;22:952-958.

Chao MJ, Ramagopalan SV, Herrera BM, Orton SM, Handunnetthi L, Lincoln MR, Dyment DA, Sadovnick AD, Ebers GC. MHC transmission insights into gender bias in MS susceptibility. Neurology 2011;76:242-246.

Chard DT, Griffin CM, Parker GJ, Kapoor R, Thompson AJ, Miller DH. Brain atrophy in clinically early relapsing-remitting multiple sclerosis. Brain 2002;125:327-337.

Clarke JT. Narrative review: Fabry disease. Ann Intern Med 2007;146:425-433.

Clerico M, Faggiano F, Palace J, Rice G, Tintoré Subiana M, Durelli L. Recombinant interferon beta or glatiramer acetate for delaying conversion of the first demyelinating event to multiple sclerosis. Cochrane Database Syst Rev 2008;16(2).

Coffey CE, Wilkinson WE, Parashos IA, Soady SAR, Sullivan RJ, Patterson LJ, Figiel GS, Webb MC, Spritzer CE, Djang WT. Quantitative cerebral anatomy of the aging human brain: a cross-sectional study using magnetic resonance-imaging. Neurology 1992;42:527-536.

Cohen JA, Barkhof F, Comi G, Hartung HP, Khatri BO, Montalban X, Pelletier J, Capra R, Gallo P, Izquierdo G, Tiel-Wilck K, de Vera A, Jin J, Stites T, Wu S, Aradhye S, Kappos L, TRANSFORMS Study Group. Oral fingolimod or intramuscular interferon for relapsing multiple sclerosis. N Engl J Med 2010;362:402-415.

Comi G, Filippi M, Wolinsky JS. European/Canadian multicenter, double-blind, randomized, placebo-controlled study of the effects of glatiramer acetate on magnetic resonance imaging-measured disease activity and burden in patients with relapsing multiple sclerosis. European/Canadian Glatiramer Acetate Study Group. Ann Neurol 2001;49:290-297.

Compston A, Coles A. Multiple sclerosis. Lancet 2002;359:1221-1231.

Compston A. Genetic epidemiology of multiple sclerosis. J Neurol Neurosurg Psychiatry 1997;62:553-561.

Confavreux C, Hutchinson M, Hours MM, Cortinovis-Tourniaire P, Moreau T, Pregnancy in Multiple Sclerosis Group. Rate of pregnancy-related relapse in multiple sclerosis. N Engl J Med 1998;339:285-291.

Confavreux C, Vukusic S. Natural history of multiple sclerosis: a unifying concept. Brain 2006;129:606-616.

Counsell SJ, Shen YJ, Boardman JP, Larkman DJ, Kapellou O, Ward P, Allsop JM, Cowan FM, Hajnal JV, Edwards AD, Rutherford MA. Axial and radial diffusivity in preterm infants who have diffuse white matter changes on magnetic resonance imaging at term-equivalent age. Pediatrics 2006;117:376-386.

Coyle PK. Pregnancy and multiple sclerosis. Neurol Clin 2012;30:877-888.

Cree BA. Multiple sclerosis. In: Brust JCM, editor. Current Diagnosis and Treatment in Neurology. New York, USA: Lange Medical Books/McGraw-Hill Medical; 2007.

Cutter GR, Baier ML, Rudick RA, Cookfair DL, Fischer JS, Petkau J, Syndulko K, Weinshenker BG, Antel JP, Confavreux C, Ellison GW, Lublin F, Miller AE, Rao SM, Reingold S, Thompson A, Willoughby E. Development of a multiple sclerosis functional composite as a clinical trial outcome measure. Brain 1999;122:871-882.

Dalton CM, Chard DT, Davies GR, Miszkiel KA, Altmann DR, Fernando K, Plant GT, Thompson AJ, Miller DH. Early development of multiple sclerosis is associated with progressive grey matter atrophy in patients presenting with clinically isolated syndromes. Brain 2004;127:1101-1107.

Daumer M, Weinshenker BG, Voskuhl R. Pregnancy: a "modifiable" risk factor in MS? Neurology 2012;78:846-848.

de Graaf WL, Kilsdonk ID, Lopez-Soriano A, Zwanenburg JJ, Visser F, Polman CH, Castelijns JA, Geurts JJ,

Pouwels PJ, Luijten PR, Barkhof F, Wattjes MP. Clinical application of multi-contrast 7-T MR imaging in multiple sclerosis: increased lesion detection compared to 3 T confined to grey matter. Eur Radiol 2013;23:528-540.

D'Hooghe MB, Nagels G, Uitdehaag BMJ. Long-term effects of childbirth in MS. J Neurol Neurosurg Psychiatry 2010;81:38-41.

Douaud G, Smith S, Jenkinson M, Behrens T, Johansen-Berg H, Vickers J, James S, Voets N, Watkins K, Matthews PM, James A. Anatomically related grey and white matter abnormalities in adolescent-onset schizophrenia. Brain 2007;130:2375-2386.

Droogan AG, Clark CA, Werring DJ, Barker GJ, McDonald WI, Miller DH. Comparison of multiple sclerosis clinical subgroups using navigated spin echo diffusion-weighted imaging. Magn Reson Imaging 1999;17:653-661.

Ebisu T, Tanaka C, Umeda M, Kitamura M, Naruse S, Higuchi T, Ueda S, Sato H. Discrimination of brain abscess from necrotic or cystic tumors by diffusion-weighted echo planar imaging. Magn Reson Imaging 1996;14:1113-1116.

Elovaara I, Airas L, Atula S, Erälinna JP, Färkkilä M, Hartikainen P, Koivisto K, Mäenpää E, Remes A, Ruutiainen J. MS-tauti. The Finnish Medical Society Duodecim, Käypä Hoito-suositus hoi36070. 2012. http://www.terveysportti.fi/xmedia/hoi/hoi36070.pdf

Engelter ST, Provenzale JM, Petrella JR. Assessment of vasogenic edema in eclampsia using diffusion imaging. Neuroradiology 2000;42:818-820.

Estes ML, Rudick RA, Barnett GH, Ransohoff RM. Stereotaxic biopsy of an active multiple-sclerosis lesion. Immunocytochemical analysis and neuropathologic correlation with magnetic resonance imaging. Arch Neurol 1990;47:1299-1303.

Fabry J. Ein Beitrag zur Kenntnis der Purpura haemorrhagica nodularis (Purpura hemorrhagica Hebrae). Arch Dermatol Syph 1898;43:187–200.

Farid N, Girard HM, Kemmotsu N, Smith ME, Magda SW, Lim WY, Lee RR, McDonald CR. Temporal lobe epilepsy: quantitative MR volumetry in detection of hippocampal atrophy. Radiology 2012;264:542-550.

Fazekas F, Chawluk JB, Alavi A, Hurtig HI, Zimmerman RA. MR signal abnormalities at 1.5 T in Alzheimer´s dementia and normal aging. AJR Am J Roentgenol 1987;149:351-356.

Fazekas F, Kleinert R, Offenbacher H, Schmidt R, Kleinert G, Payer F, Radner H, Lechner H. Pathological correlates of incidental MRI white-matter signal hyperintensities. Neurology 1993;43:1683-1689.

Fellgiebel A, Keller I, Martus P, Ropele S, Yakushev I, Böttcher T, Fazekas F, Rolfs A. Basilar artery diameter is a potential screening tool for Fabry disease in young stroke patients. Cerebrovasc Dis 2011;31:294-299.

Fellgiebel A, Mazanek M, Whybra C, Beck M, Hartung R, Müller KM, Scheurich A, Dellani PR, Stoeter P, Müller MJ. Pattern of microstructural brain tissue alterations in Fabry disease - a diffusion-tensor imaging study. J Neurol 2006a;253:780-787.

Fellgiebel A, Müller MJ, Ginsberg L. CNS manifestations of Fabry's disease. Lancet Neurol 2006b;5:791-795.

Fernando KT, Tozer DJ, Miszkiel KA, Gordon RM, Swanton JK, Dalton CM, Barker GJ, Plant GT, Thompson AJ, Miller DH. Magnetization transfer histograms in clinically isolated syndromes suggestive of multiple sclerosis. Brain 2005;128:2911-2925.

Filippi M, Iannucci G, Cercignani M, Assunta Rocca M, Pratesi A, Comi G. A quantitative study of water diffusion in multiple sclerosis lesions and normal-appearing white matter using echo-planar imaging. Arch Neurol 2000;57:1017-1021.

Finkelsztejn A, Fragoso YD, Ferreira ML, Lana-Peixoto MA, Alves-Leon SV, Gomes S, Damasceno BP, Mendes MF, Salgado PR, Correa EC, Comini-Frota ER, Diniz DS, Gama PD, Kaimen-Maciel DR, Morales RR, Arruda WO, Grzesiuk AK, Khouri JM, Lopes JS, Rocha CF, Domingues R, Gonçalves MV, Lorenti MA, Parolin MK, Siquineli F, Tosta ED, Brooks JB, Gallina AS, Melges LD, Ruocco HH. The Brazilian database on pregnancy in multiple sclerosis. Clin Neurol Neurosurg 2011;113:277-280.

Fisher E, Rudick RA, Simon JH, Cutter G, Baier M, Lee JC, Miller D, Weinstock-Guttman B, Mass MK, Dougherty DS, Simonian NA. Eight-year follow-up study of brain atrophy in patients with MS. Neurology 2002;59:1412-1420.

Focke NK, Yogarajah M, Bonelli SB, Bartlett PA, Symms MR, Duncan JS. Voxel-based diffusion tensor imaging in patients with mesial temporal lobe epilepsy and hippocampal sclerosis. Neuroimage 2008;40:728-737.

Francis G, Hughes R, King J, Mitchell P, Joubert J, McLeod J, Parker G, Pollard J, Sindic CJ, Duprez T, Medaer R, Broeckx J, Vanroose E, Carton H, Wilms G, Rice G, Ebers G, Lee DH, Freedman M, Nelson R, Rabinovitch H, Christie S, Avruch L, Oger J, Paty DW, Li D, Wikström J, Salonen OL, Panelius M, Erälinna J, Sonninen P, Rieckmann P, Hahn D, Flachenecker P, Hartung HP, Uitdehaag B, Bertelsmann FW, Barkhof F, Hommes OR, Jongen PJ, Van Doorn PA, Tanghe HL, Sandberg-Wollheim M, Larsson EM, Lönntoft M, Sallerfors S, Kappos L, Lienert C, Radü EW, Chofflon M, Roth S, Castillo V, Schwieger AF, Hughes RAC, Clews AM, Bingham JB, Barnes D, Clifton AG, Stoy N, Bates D, Coulthard A, Blumhardt LD, Evans SM, Jaspan T, Palace J, Newsom-Davis JM, Byrne JV, Quaghebeur G, Li DKB, Zhao GJ, Riddehough A, Rhodes B; PRISMS Study Group; University of British Columbia MS/MRI Analysis Group. Long-term efficacy

of interferon-beta-1a in relapsing MS. Neurology 2001;56:1628-1636.

Gallo A, Rovaris M, Riva R, Angelo GI, Benedetti B, Martinelli V, Falini A, Comi G, Filippi M. Diffusion-tensor magnetic resonance imaging detects normal-appearing white matter damage unrelated to short-term disease activity in patients at the earliest clinical stage of multiple sclerosis. Arch Neurol 2005;62:803-808.

Garaci FG, Colangelo V, Ludovici A, Gaudiello F, Marziali S, Centonze D, Boffa L, Simonetti G, Floris R. A diffusion longitudinal MR imaging study in normal-appearing white matter in untreated relapsing-remitting multiple sclerosis. AJNR Am J Neuroradiol 2007;28:475-478.

Gass A, Niendorf T, Hirsch JG. Acute and chronic changes of the apparent diffusion coefficient in neurological disorders - biophysical mechanisms and possible underlying histopathology. J Neurol Sci 2001;186 Suppl1:S15-S23.

Ge YL, Grossman RI, Udupa JK, Babb JS, Nyúl LG, Kolson DL. Brain atrophy in relapsing-remitting multiple sclerosis: fractional volumetric analysis of gray matter and white matter. Radiology 2001;220:606-610.

Gerstner ER, Sorensen AG. Diffusion and diffusion tensor imaging in brain cancer. Semin Radiat Oncol 2011;21:141-146.

Gold R, Buttgereit F, Toyka KV. Mechanism of action of glucocorticosteroid hormones: possible implications for therapy of neuroimmunological disorders. J Neuroimmunol 2001;117:1-8.

Good CD, Johnsrude IS, Ashburner J, Henson RN, Friston KJ, Frackowiak RS. A voxel-based morphometric study of ageing in 465 normal adult human brains. Neuroimage 2001;14:21-36.

Grossman RI, Gonzalez-Scarano F, Atlas SW, Galetta S, Silberberg DH. Multiple sclerosis: gadolinium enhancement in MR imaging. Radiology 1986;161:721-725.

Harris AD, Coutts SB, Frayne R. Diffusion and perfusion MR imaging of acute ischemic stroke. Magn Reson Imaging Clin N Am 2009;17:291-313.

Hedström AK, Åkerstedt T, Hillert J, Olsson T, Alfredsson L. Shift work at young age is associated with increased risk for multiple sclerosis. Ann Neurol 2011a; 70:733-741.

Hedström AK, Bäärnhielm M, Olsson T, Alfredsson L. Exposure to environmental tobacco smoke is associated with increased risk for multiple sclerosis. Mult Scler 2011b;17:788-793.

Hedström AK, Bäärnhielm M, Olsson T, Alfredsson L. Tobacco smoking, but not swedish snuff use, increases the risk of multiple sclerosis. Neurology 2009;73:696-701.

Hernán MA, Jick SS, Logroscino G, Olek MJ, Ascherio A, Jick H. Cigarette smoking and the progression of multiple sclerosis. Brain 2005;128:1461-1465.

Hernán MA, Olek MJ, Ascherio A. Cigarette smoking and incidence of multiple sclerosis. Am J Epidemiol 2001;154:69-74.

Hobart J, Lamping D, Fitzpatrick R, Riazi A, Thompson A. The Multiple Sclerosis Impact Scale (MSIS-29) - a new patient-based outcome measure. Brain 2001;124:962-973.

Horsfield MA, Larsson HB, Jones DK, Gass A. Diffusion magnetic resonance imaging in multiple sclerosis. J Neurol Neurosurg Psychiatry 1998;64 Suppl 1:S80-S84.

Hussien Y, Sanna A, Söderstrom M, Link H, Huang YM. Glatiramer acetate and IFN-beta act on dendritic cells in multiple sclerosis. J Neuroimmunol 2001;121:102-110.

Iwashiro N, Suga M, Takano Y, Inoue H, Natsubori T, Satomura Y, Koike S, Yahata N, Murakami M, Katsura M, Gonoi W, Sasaki H, Takao H, Abe O, Kasai K, Yamasue H. Localized gray matter volume reductions in the pars triangularis of the inferior frontal gyrus in individuals at clinical high-risk for psychosis and first episode for schizophrenia. Schizophr Res 2012;137:124-131.

Jacobs LD, Beck RW, Simon JH, Kinkel RP, Brownscheidle CM, Murray TJ, Simonian NA, Slasor PJ, Sandrock AW. Intramuscular interferon beta-1a therapy initiated during a first demyelinating event in multiple sclerosis. CHAMPS Study Group. N Engl J Med 2000;343:898-904.

Jenkinson M, Bannister P, Brady M, Smith S. Improved optimization for the robust and accurate linear registration and motion correction of brain images. Neuroimage 2002;17:825-841.

Jenkinson M, Smith S. A global optimisation method for robust affine registration of brain images. Med Image Anal 2001;5:143-156.

Joutsa J, Saunavaara J, Parkkola R, Niemelä S, Kaasinen V. Extensive abnormality of brain white matter integrity in pathological gambling. Psychiatry Res 2011;194:340-346.

Kalincik T, Vaneckova M, Tyblova M, Krasensky J, Seidl Z, Havrdova E, Horakova D. Volumetric MRI markers and predictors of disease activity in early multiple sclerosis: a longitudinal cohort study. PLoS One 2012;7(11).

Kalkers NF, Ameziane N, Bot JC, Minneboo A, Polman CH, Barkhof F. Longitudinal brain volume measurement in multiple sclerosis: rate of brain atrophy is independent of the disease subtype. Arch Neurol 2002;59:1572-1576.

Kampmann C, Linhart A, Baehner F, Palecek T, Wiethoff CM, Miebach E, Whybra C, Gal A, Bultas J, Beck M.

Onset and progression of the Anderson-Fabry disease related cardiomyopathy. Int J Cardiol 2008;130:367-373.

Kantola I, Penttinen M, Nuutila P, Viikari J. Fabryn tauti. Duodecim, 2012;128:729-739.

Kappos L, Freedman MS, Polman CH, Edan G, Hartung HP, Miller DH, Montalbán X, Barkhof F, Radü EW, Bauer L, Dahms S, Lanius V, Pohl C, Sandbrink R, BENEFIT Study Group. Effect of early versus delayed interferon beta-1b treatment on disability after a first clinical event suggestive of multiple sclerosis: a 3-year follow-up analysis of the BENEFIT study. Lancet 2007;370:389-397.

Khalil RA, Crews JK, Novak J, Kassab S, Granger JP. Enhanced vascular reactivity during inhibition of nitric oxide synthesis in pregnant rats. Hypertension 1998;31:1065-1069.

Kidd D, Barkhof F, McConnell R, Algra PR, Allen IV, Revesz T. Cortical lesions in multiple sclerosis. Brain 1999;122:17-26.

Kister I, Chamot E, Salter AR, Cutter GR, Bacon TE, Herbert J. Disability in multiple sclerosis. A reference for patients and clinicians. Neurology 2013;80:1018-1024.

Koch S, Rabinstein A, Falcone S, Forteza A. Diffusion-weighted imaging shows cytotoxic and vasogenic edema in eclampsia. AJNR Am J Neuroradiol 2001;22:1068-1070.

Koralnik IJ. New insights into progressive multifocal leukoencephalopathy. Curr Opin Neurol 2004;17:365-370.

Kurtzke JF. Geography in multiple sclerosis. J Neurol 1977;215:1-26.

Kurtzke JF. Rating neurologic impairment in multiple sclerosis: an expanded disability status scale (EDSS). Neurology 1983;33:1444-1452.

Langer-Gould A, Atlas SW, Green AJ, Bollen AW, Pelletier D: Progressive multifocal leukoencephalopathy in a patient treated with natalizumab. N Engl J Med 2005;353:375-381.

Le Bihan D, Mangin JF, Poupon C, Clark CA, Pappata S, Molko N, Chabriat H: Diffusion tensor imaging: concepts and applications. J Magn Reson Imaging 2001;13:534-546.

Lepomäki V, Matomäki J, Lapinleimu H, Lehtonen L, Haataja L, Komu M, Parkkola R; PIPARI Study Group. Effect of antenatal growth on brain white matter maturation in preterm infants at term using tract-based spatial statistics. Pediatr Radiol 2013;43:80-85.

Lepomäki VK, Paavilainen TP, Hurme SA, Komu ME, Parkkola RK; PIPARI Study Group. Fractional anisotropy and mean diffusivity parameters of the brain white matter tracts in preterm infants: reproducibility of region-of-interest measurements. Pediatr Radiol 2012;42:175-182.

Leppert D, Waubant E, Bürk MR, Oksenberg JR, Hauser SL. Interferon beta-1b inhibits gelatinase secretion and in vitro migration of human T cells: a possible mechanism for treatment efficacy in multiple sclerosis. Ann Neurol 1996;40:846-852.

Li CM, Du HJ, Zheng J, Wang J. A voxel-based morphometric analysis of cerebral gray matter in subcortical ischemic vascular dementia patients and normal aged controls. Int J Med Sci 2011;8:482-486.

Li DK, Paty DW, the UBC MS/MRI Analysis Research Group, the PRISMS Study Group. Magnetic resonance imaging results of the PRISMS trial: A randomized, double-blind, placebo-controlled study of interferon-beta 1a in relapsing-remitting multiple sclerosis. Ann Neurol 1999;46:197-206.

Lillo P, Mioshi E, Burrell JR, Kiernan MC, Hodges JR, Hornberger M. Grey and white matter changes across the amyotrophic lateral sclerosis-frontotemporal dementia continuum. PLoS One 2012;7(8).

Lin Y, Wang J, Wu C, Wai Y, Yu J, Ng S. Diffusion tensor imaging of the auditory pathway in sensorineural hearing loss: changes in radial diffusivity and diffusion anisotropy. J Magn Reson Imaging 2008;28:598-603.

Liu AY, Maldjian JA, Bagley LJ, Sinson GP, Grossman RI. Traumatic brain injury: diffusion-weighted MR imaging findings. AJNR Am J Neuroradiol 1999;20:1636-1641.

Liu YW, Spulber G, Lehtimaki KK, Könönen M, Hallikainen I, Gröhn H, Kivipelto M, Hallikainen M, Vanninen R, Soininen H. Diffusion tensor imaging and Tract-Based Spatial Statistics in Alzheimer's disease and mild cognitive impairment. Neurobiol Aging 2011;32:1558-1571.

Llufriu S, Blanco Y, Martinez-Heras E, Casanova-Molla J, Gabilondo I, Sepulveda M, Falcon C, Berenguer J, Bargallo N, Villoslada P, Graus F, Valls-Sole J, Saiz A. Influence of corpus callosum damage on cognition and physical disability in multiple sclerosis: a multimodal study. PLoS One 2012;7:e37167.

Lou X, Jiang WJ, Ma L, Ma N, Cai Y, Huang D, Wong EH. Lower fractional anisotropy at the anterior body of the normal-appearing corpus callosum in multiple sclerosis versus symptomatic carotid occlusion. Neuroradiology 2009;51:557-561.

Lublin FD, Reingold SC. Defining the clinical course of multiple sclerosis: results of an international survey. National Multiple Sclerosis Society (USA) Advisory Committee on Clinical Trials of New Agents in Multiple Sclerosis. Neurology 1996;46:907-911.

Luks TL, Goodkin DE, Nelson SJ, Majumdar S, Bacchetti P, Portnoy D, Sloan R. A longitudinal study of ventricular volume in early relapsing-remining multiple sclerosis. Mult Scler 2000;6:332-337.

MacDermot KD, Holmes A, Miners AH. Anderson-Fabry disease: clinical manifestations and impact of disease in a cohort of 60 obligate carrier females. J Med Genet 2001;38:769-775.

Marenco S, Rawlings R, Rohde GK, Barnett AS, Hone RA, Pierpaoli C, Weinberger DR. Regional distribution of measurement error in diffusion tensor imaging. Psychiatry Res 2006;147:69-78.

Mascalchi M, Lolli F, Della Nave R, Tessa C, Petralli R, Gavazzi C, Politi LS, Macucci M, Filippi M, Piacentini S. Huntington disease: volumetric, diffusion-weighted, and magnetization transfer MR imaging of brain. Radiology 2004;232:867-873.

Mascalchi M, Tessa C, Moretti M, Della Nave R, Boddi V, Martini S, Inzitari D, Villari N. Whole brain apparent diffusion coefficient histogram: a new tool for evaluation of leukoaraiosis. J Magn Reson Imaging 2002;15:144-148.

McDonald WI, Compston A, Edan G, Goodkin D, Hartung HP, Lublin FD, McFarland HF, Paty DW, Polman CH, Reingold SC, Sandberg-Wollheim M, Sibley W, Thompson AJ, van den Noort S, Weinshenker BY, Wolinsky JS. Recommended diagnostic criteria for multiple sclerosis: guidelines from the International Panel on the diagnosis of multiple sclerosis. Ann Neurol 2001;50:121-127.

Messiano S, Jaffe RB. The endocrinology of human pregnancy and fetal-placental neuroendocrine development. In: Strauss JF, Barbieri R, editors. Yen and Jaffe´s Reproductive Endocrinology. Philadelphia, USA: Saunders Company, 2004:745-767.

Miller DH, Thompson AJ, Morrissey SP, MacManus DG, Moore SG, Kendall BE, Moseley IF, McDonald WI. High dose steroids in acute relapses of multiple-sclerosis: MRI evidence for a possible mechanism of therapeutic effect. J Neurol Neurosurg Psychiatry 1992;55:450-453.

Miller DH, Weinshenker BG, Filippi M, Banwell BL, Cohen JA, Freedman MS, Galetta SL, Hutchinson M, Johnson RT, Kappos L, Kira J, Lublin FD, McFarland HF, Montalban X, Panitch H, Richert JR, Reingold SC, Polman CH. Differential diagnosis of suspected multiple sclerosis: A consensus approach. Mult Scler 2008;14:1157-1174.

Miller DM, Weinstock-Guttman B, Béthoux F, Lee JC, Beck G, Block V, Durelli L, LaMantia L, Barnes D, Sellebjerg F, Rudick RA. A meta-analysis of methylprednisolone in recovery from multiple sclerosis exacerbations. Mult Scler 2000;6:267-273.

Minamikawa S, Kono K, Nakayama K, Yokote H, Tashiro T, Nishio A, Hara M, Inoue Y. Glucocorticoid treatment of brain tumor patients. changes of apparent diffusion coefficient values measured by MR diffusion imaging. Neuroradiology 2004;46:805-811.

Moore DF, Altarescu G, Barker WC, Patronas NJ, Herscovitch P, Schiffmann R. White matter lesions in Fabry disease occur in 'prior' selectively hypometabolic and hyperperfused brain regions. Brain Res Bull 2003;62:231-240.

Moore DF, Schiffmann R, Ulug AM. Elevated CNS average diffusion constant in Fabry disease. Acta Paediatr Suppl 2002;91:67-68.

Morales Y, Parisi JE, Lucchinetti CF. The Pathology of Multiple Sclerosis: Evidence for Heterogeneity. In: Freedman MS, editor. Advances in Neurology. Multiple Sclerosis and Demyelinating Diseases. 98th vol. Philadelphia, USA: Lippincott Williams & Wilkins; 2006.

Mowry EM, Krupp LB, Milazzo M, Chabas D, Strober JB, Belman AL, McDonald JC, Oksenberg JR, Bacchetti P, Waubant E. Vitamin D status is associated with relapse rate in pediatric-onset multiple sclerosis. Ann Neurol 2010;67:618-624.

Mowry EM, Waubant E, McCulloch CE, Okuda DT, Evangelista AA, Lincoln RR, Gourraud PA, Brenneman D, Owen MC, Qualley P, Bucci M, Hauser SL, Pelletier D. Vitamin D status predicts new brain magnetic resonance imaging activity in multiple sclerosis. Ann Neurol 2012;72:234-240.

Mueller SG, Schuff N, Yaffe K, Madison C, Miller B, Weiner MW. Hippocampal atrophy patterns in mild cognitive impairment and Alzheimer's disease. Hum Brain Mapp 2010;31:1339-1347.

Mukherjee P, Chung SW, Berman JI, Hess CP, Henry RG. Diffusion tensor MR imaging and fiber tractography: technical considerations. AJNR Am J Neuroradiol 2008;29:843-852.

Müller M, Frese A, Nassenstein I, Hoppen M, Marziniak M, Ringelstein EB, Kim KS, Schäbitz WR, Kraus J. Serum from interferon-β-1b-treated patients with early multiple sclerosis stabilizes the blood-brain barrier in vitro. Mult Scler 2012;18:236-239.

Munger KL, Zhang SM, O'Reilly E, Hernán MA, Olek MJ, Willett WC, Ascherio A. Vitamin D intake and incidence of multiple sclerosis. Neurology 2004;62:60-65.

Myers C, Duncan KR, Gowland PA, Johnson IR, Baker PN. Failure to detect intrauterine growth restriction following in utero exposure to MRI. Br J Radiol 1998;71:549-551.

Neil JJ. Diffusion imaging concepts for clinicians. J Magn Reson Imaging 2008;27:1-7.

Nesbit GM, Forbes GS, Scheithauer BW, Okazaki H, Rodriguez M. Multiple sclerosis: histopathologic and MR and/or CT correlation in 37 cases at biopsy and 3 cases at autopsy. Radiology 1991;180:467-474.

Nichols TE, Holmes AP. Nonparametric permutation tests for functional neuroimaging: a primer with examples. Hum Brain Mapp 2002;15:1-25.

Niemelä J, Ifergan I, Yegutkin GG, Jalkanen S, Prat A, Airas L. IFN-beta regulates CD73 and adenosine expression at the blood-brain barrier. Eur J Immunol 2008;38:2718-2726.

Noseworthy JH, Lucchinetti C, Rodriguez M, Weinshenker BG. Multiple sclerosis. N Engl J Med 2000;343:938-952.

Nucifora PG, Verma R, Lee SK, Melhem ER. Diffusion-tensor MR imaging and tractography: exploring brain microstructure and connectivity. Radiology 2007;245:367-384.

Okeda R, Nisihara M. An autopsy case of Fabry disease with neuropathological investigation of the pathogenesis of associated dementia. Neuropathology 2008;28:532-540.

Oreja-Guevara C, Rovaris M, Iannucci G, Valsasina P, Caputo D, Cavarretta R, Sormani MP, Ferrante P, Comi G, Filippi M. Progressive gray matter damage in patients with relapsing-remitting multiple sclerosis: a longitudinal diffusion tensor magnetic resonance imaging study. Arch Neurol 2005;62:578-584.

Ormerod IEC, Miller DH, McDonald WI, du Boulay E, Rudge P, Kendall BE, Moseley IF, Johnson G, Tofts PS, Halliday AM, Bronstein AM, Scaravilli F, Harding AE, Barnes D, Zilkha KJ. The role of NMR imaging in the assessment of multiple-sclerosis and isolated neurological lesions. A quantitative study. Brain 1987;110:1579-1616.

Ortiz A, Cianciaruso B, Cizmarik M, Germain DP, Mignani R, Oliveira JP, Villalobos J, Vujkovac B, Waldek S, Wanner C, Warnock DG. End-stage renal disease in patients with Fabry disease: Natural history data from the Fabry Registry. Nephrol Dial Transplant 2010;25:769-775.

Ortiz A, Oliveira JP, Waldek S, Warnock DG, Cianciaruso B, Wanner C; Fabry Registry. Nephropathy in males and females with Fabry disease: cross-sectional description of patients before treatment with enzyme replacement therapy. Nephrol Dial Transplant 2008;23:1600-1607.

Ozturk A, Sasson AD, Farrell JAD, Landman BA, da Motta A, Aralasmak A, Yousem DM. Regional differences in diffusion tensor imaging measurements: assessment of intrarater and interrater variability. AJNR Am J Neuroradiol 2008;29:1124-1127.

Pagani E, Rocca MA, Gallo A, Rovaris M, Martinelli V, Comi G, Filippi M. Regional brain atrophy evolves differently in patients with multiple sclerosis according to clinical phenotype. AJNR Am J Neuroradiol 2005;26:341-346.

Parini R, Rigoldi M, Santus F, Furlan F, De Lorenzo P, Valsecchi G, Concolino D, Strisciuglio P, Feriozzi S, Di Vito R, Ravaglia R, Ricci R, Morrone A. Enzyme replacement therapy with agalsidase alfa in a cohort of Italian patients with Anderson-Fabry disease: testing the effects with the Mainz Severity Score Index. Clin Genet 2008;74:260-266.

Pfefferbaum A, Mathalon DH, Sullivan EV, Rawles JM, Zipursky RB, Lim KO. A quantitative magnetic resonance imaging study of changes in brain morphology from infancy to late adulthood. Arch Neurol 1994;51:874-887.

Pierpaoli C, Basser PJ. Toward a quantitative assessment of diffusion anisotropy. Magn Reson Med 1996;36:893-906.

Polman CH, O'Connor PW, Havrdova E, Hutchinson M, Kappos L, Miller DH, Phillips JT, Lublin FD, Giovannoni G, Wajgt A, Toal M, Lynn F, Panzara MA, Sandrock AW, AFFIRM Investigators. A randomized, placebo-controlled trial of natalizumab for relapsing multiple sclerosis. N Engl J Med 2006;354:899-910.

Polman CH, Reingold SC, Banwell B, Clanet M, Cohen JA, Filippi M, Fujihara K, Havrdova E, Hutchinson M, Kappos L, Lublin FD, Montalban X, O'Connor P, Sandberg-Wollheim M, Thompson AJ, Waubant E, Weinshenker B, Wolinsky JS. Diagnostic criteria for multiple sclerosis: 2010 revisions to the McDonald criteria. Ann Neurol 2011;69:292-302.

Polman CH, Reingold SC, Edan G, Filippi M, Hartung HP, Kappos L, Lublin FD, Metz LM, McFarland HF, O'Connor PW, Sandberg-Wollheim M, Thompson AJ, Weinshenker BG, Wolinsky JS. Diagnostic criteria for multiple sclerosis: 2005 revisions to the "McDonald Criteria". Ann Neurol 2005;58:840-846.

Ponsonby AL, Lucas RM, van der Mei IA, Dear K, Valery PC, Pender MP, Taylor BV, Kilpatrick TJ, Coulthard A, Chapman C, Williams D, McMichael AJ, Dwyer T. Offspring number, pregnancy, and risk of a first clinical demyelinating event: the AusImmune study. Neurology 2012;78:867-874.

Provenzale JM, Liang L, DeLong D, White LE. Diffusion tensor imaging assessment of brain white matter maturation during the first postnatal year. AJR Am J Roentgenol 2007;189:476-486.

Ramaswami U, Whybra C, Parini R, Pintos-Morell G, Mehta A, Sunder-Plassmann G, Widmer U, Beck M; FOS European Investigators. Clinical manifestations of Fabry disease in children: data from the Fabry Outcome Survey. Acta Paediatr 2006;95:86-92.

Reeves MJ, Brandreth M, Whitby EH, Hart AR, Paley MN, Griffiths PD, Stevens JC. Neonatal cochlear function: measurement after exposure to acoustic noise during in utero MR imaging. Radiology 2010;257:802-809.

Reisin RC, Romero C, Marchesoni C, Nápoli G, Kisinovsky I, Cáceres G, Sevlever G. Brain MRI

findings in patients with Fabry disease. J Neurol Sci 2011;305:41-44.

Riise T, Nortvedt MW, Ascherio A. Smoking is a risk factor for multiple sclerosis. Neurology 2003;61:1122-1124.

Rizzo G, Manners D, Vetrugno R, Tonon C, Malucelli E, Plazzi G, Marconi S, Pizza F, Testa C, Provini F, Montagna P, Lodi R. Combined brain voxel-based morphometry and diffusion tensor imaging study in Idiopathic Restless Legs Syndrome patients. Eur J Neurol 2012;19:1045-1049.

Rocca MA, Cercignani M, Iannucci G, Comi G, Filippi M. Weekly diffusion-weighted imaging of normal-appearing white matter in MS. Neurology 2000;55:882-884.

Roosendaal SD, Geurts JJG, Vrenken H, Hulst HE, Cover KS, Castelijns JA, Pouwels PJW, Barkhof F. Regional DTI differences in multiple sclerosis patients. Neuroimage 2009;44:1397-1403.

Roullet E, Verdier-Taillefer MH, Amarenco P, Gharbi G, Alperovitch A, Marteau R. Pregnancy and multiple-sclerosis: a longitudinal-study of 125 remittent patients. J Neurol Neurosurg Psychiatry 1993;56:1062-1065.

Rovaris M, Bozzali M, Iannucci G, Ghezzi A, Caputo D, Montanari E, Bertolotto A, Bergamaschi R, Capra R, Mancardi GL, Martinelli V, Comi G, Filippi M. Assessment of normal-appearing white and gray matter in patients with primary progressive multiple sclerosis: a diffusion-tensor magnetic resonance imaging study. Arch Neurol 2002;59:1406-1412.

Rovaris M, Judica E, Gallo A, Benedetti B, Sormani MP, Caputo D, Ghezzi A, Montanari E, Bertolotto A, Mancardi G, Bergamaschi R, Martinelli V, Comi G, Filippi M. Grey matter damage predicts the evolution of primary progressive multiple sclerosis at 5 years. Brain 2006;129:2628-2634.

Roxburgh R, Seaman SR, Masterman T, Hensiek AE, Sawcer SJ, Vukusic S, Achiti I, Confavreux C, Coustans M, le Page E, Edan G, McDonnell GV, Hawkins S, Trojano M, Liguori M, Cocco E, Marrosu MG, Tesser F, Leone MA, Weber A, Zipp F, Miterski B, Epplen JT, Oturai A, Sørensen PS, Celius EG, Lara NT, Montalban X, Villoslada P, Silva AM, Marta M, Leite I, Dubois B, Rubio J, Butzkueven H, Kilpatrick T, Mycko MP, Selmaj KW, Rio ME, Sá M, Salemi G, Savettieri G, Hillert J, Compston DAS. Multiple Sclerosis Severity Score - using disability and disease duration to rate disease severity. Neurology 2005;64:1144-1151.

Roychowdhury S, Maldjian JA, Grossman RI. Multiple sclerosis: comparison of trace apparent diffusion coefficients with MR enhancement pattern of lesions. AJNR Am J Neuroradiol 2000;21:869-874.

Rueckert D, Sonoda LI, Hayes C, Hill DG, Leac MO, Hawkes DJ. Non-rigid registration using free-form deformations: application to breast MR images. IEEE Trans Med Imaging 1999;20:712-721.

Runmarker B, Andersen O. Pregnancy is associated with a lower risk of onset and a better prognosis in multiple-sclerosis. Brain 1995;118:253-261.

Sadovnick AD, Eisen K, Hashimoto SA, Farquhar R, Yee IM, Hooge J, Kastrukoff L, Oger JJ, Paty DW. Pregnancy and multiple-sclerosis. A prospective study. Arch Neurol 1994;51:1120-1124.

Saksena S, Husain N, Malik GK, Trivedi R, Sarma M, Rathore RS, Pandey CM, Gupta RK. Comparative evaluation of the cerebral and cerebellar white matter development in pediatric age group using quantitative diffusion tensor imaging. Cerebellum 2008;7:392-400.

Sämann PG, Knop M, Golgor E, Messler S, Czisch M, Weber F. Brain volume and diffusion markers as predictors of disability and short-term disease evolution in multiple sclerosis. AJNR Am J Neuroradiol 2012;33:1356-1362.

Saraste MH, Kurki T, Airas LM. Postpartum activation of multiple sclerosis: MRI imaging and immunological characterization of a case. Eur J Neurol 2006;13:98-99.

Scalfari A, Neuhaus A, Degenhardt A, Rice GP, Muraro PA, Daumer M, Ebers GC. The natural history of multiple sclerosis, a geographically based study 10: Relapses and long-term disability. Brain 2010;133:1914-1929.

Schaefer PW, Buonanno FS, Gonzalez RG, Schwamm LH. Diffusion-weighted imaging discriminates between cytotoxic and vasogenic edema in a patient with eclampsia. Stroke 1997;28:1082-1085.

Schaefer PW, Grant PE, Gonzalez RG. Diffusion-weighted MR imaging of the brain. Radiology 2000;217:331-345.

Schiffmann R, Kopp JB, Austin HA 3rd, Sabnis S, Moore DF, Weibel T, Balow JE, Brady RO. Enzyme replacement therapy in Fabry disease: a randomized controlled trial. JAMA 2001;285:2743-2749.

Schiffmann R, Warnock DG, Banikazemi M, Bultas J, Linthorst GE, Packman S, Sorensen SA, Wilcox WR, Desnick RJ. Fabry disease: progression of nephropathy, and prevalence of cardiac and cerebrovascular events before enzyme replacement therapy. Nephrol Dial Transplant 2009;24:2102-2111.

Seidman LJ, Biederman J, Liang LC, Valera EM, Monuteaux MC, Brown A, Kaiser J, Spencer T, Faraone SV, Makris N. Gray matter alterations in adults with attention-deficit/hyperactivity disorder identified by voxel based morphometry. Biol Psychiatry 2011;69:857-866.

Sepulcre J, Sastre-Garriga J, Cercignani M, Ingle GT, Miller DH, Thompson AJ. Regional gray matter atrophy in early primary progressive multiple sclerosis: a voxel-

based morphometry study. Arch Neurol 2006;63:1175-1180.

Sharief MK, Semra YK, Seidi OA, Zoukos Y. Interferon-beta therapy downregulates the anti-apoptosis protein FLIP in T cells from patients with multiple sclerosis. J Neuroimmunol 2001;120:199-207.

Shellock FG, Morisoli S, Kanal E. MR procedures and biomedical implants, materials, and devices: 1993 update. Radiology 1993;189:587-599.

Simon B, Schmidt S, Lukas C, Gieseke J, Träber F, Knol DL, Willinek WA, Geurts JJ, Schild HH, Barkhof F, Wattjes MP. Improved in vivo detection of cortical lesions in multiple sclerosis using double inversion recovery MR imaging at 3 Tesla. Eur Radiol 2010;20:1675-1683.

Simon JH, Jacobs LD, Campion M, Wende K, Simonian N, Cookfair DL, Rudick RA, Herndon RM, Richert JR, Salazar AM, Alam JJ, Fischer JS, Goodkin DE, Granger CV, Lajaunie M, Martens-Davidson AL, Meyer MJ, Sheeder J, Choi K, Scherzinger AL, Bartoszak DM, Bourdette DN, Braiman J, Brownscheidle CM, Coats ME, Cohan SL, Dougherty DS, Kinkel RP, Mass MK, Munschauer FE, Priore RL, Pullicino PM, Scherokman BJ, Weinstock-Guttman B, Whitham RH. Magnetic resonance studies of intramuscular interferon beta-1a for relapsing multiple sclerosis. The Multiple Sclerosis Collaborative Research Group. Ann Neurol 1998;43:79-87.

Sirrs SM, West ML, Flowerdew G, Lemoine K, Bichet D, Casey R, Clarke J, Auray-Blais C. The Canadian Fabry Disease Initiative: a randomized controlled trial of agalsidase therapy in Fabry disease. Abstract in 11th International Congress of Inborn Errors of Metabolism, San Diego, USA, 29.8.-2.9.2009.

Smith SM, De Stefano N, Jenkinson M, Matthews PM. Normalized accurate measurement of longitudinal brain change. J Comput Assist Tomogr 2001;25:466-475.

Smith SM, Jenkinson M, Johansen-Berg H, Rueckert D, Nichols TE, Mackay CE, Watkins KE, Ciccarelli O, Cader MZ, Matthews PM, Behrens TE. Tract-based spatial statistics: Voxelwise analysis of multi-subject diffusion data. Neuroimage 2006;31:1487-1505.

Smith SM, Jenkinson M, Woolrich MW, Beckmann CF, Behrens TEJ, Johansen-Berg H, Bannister PR, De Luca M, Drobnjak I, Flitney DE, Niazy RK, Saunders J, Vickers J, Zhang YY, De Stefano N, Brady JM, Matthews PM. Advances in functional and structural MR image analysis and implementation as FSL. Neuroimage 2004;23 Suppl1:S208-S219.

Smith SM, Johansen-Berg H, Jenkinson M, Rueckert D, Nichols TE, Miller KL, Robson MD, Jones DK, Klein JC, Bartsch AJ, Behrens TE. Acquisition and voxelwise analysis of multi-subject diffusion data with tract-based spatial statistics. Nat Protoc 2007a;2:499-503.

Smith SM, Nichols TE. Threshold-free cluster enhancement: addressing problems of smoothing, threshold dependence and localisation in cluster inference. Neuroimage 2009;44:83-98.

Smith SM, Rao A, De Stefano N, Jenkinson M, Schott JM, Matthews PM, Fox NC. Longitudinal and cross-sectional analysis of atrophy in Alzheimer's disease: cross-validation of BSI, SIENA and SIENAX. Neuroimage 2007b;36:1200-1206.

Smith SM, Zhang YY, Jenkinson M, Chen J, Matthews PM, Federico A, De Stefano N. Accurate, robust, and automated longitudinal and cross-sectional brain change analysis. Neuroimage 2002;17:479-489.

Smith SM. Fast robust automated brain extraction. Hum Brain Mapp 2002;17:143-155.

Song SK, Sun SW, Ramsbottom MJ, Chang C, Russell J, Cross AH. Dysmyelination revealed through MRI as increased radial (but unchanged axial) diffusion of water. Neuroimage 2002;17:1429-1436.

Spada M, Pagliardini S, Yasuda M, Tukel T, Thiagarajan G, Sakuraba H, Ponzone A, Desnick RJ. High incidence of later-onset Fabry disease revealed by newborn screening. Am Journal Human Genet 2006;79:31-40.

Steens SC, Admiraal-Behloul F, Schaap JA, Hoogenraad FG, Wheeler-Kingshott CA, le Cessie S, Tofts PS, van Buchem MA. Reproducibility of brain ADC histograms. Eur Radiol 2004;14:425-430.

Stewart WA, Hall LD, Berry K, Churg A, Oger J, Hashimoto SA, Paty DW. Magnetic resonance imaging (MRI) in multiple-sclerosis (MS): Pathological correlation studies in eight cases. Neurology 1986;36(Suppl 1):320.

Sumelahti ML, Tienari PJ, Wikström J, Palo J, Hakama M. Increasing prevalence of multiple sclerosis in finland. Acta Neurol Scand 2001;103:153-158.

Sumelahti ML, Tienari PJ, Wikström J, Palo J, Hakama M. Regional and temporal variation in the incidence of multiple sclerosis in finland 1979-1993. Neuroepidemiology 2000;19:67-75.

Tedeschi G, Bonavita S, Banerjee TK, Virta A, Schiffmann R. Diffuse central neuronal involvement in Fabry disease: a proton MRS imaging study. Neurology 1999;52:1663-1667.

Tedeschi G, Lavorgna L, Russo P, Prinster A, Dinacci D, Savettieri G, Quattrone A, Livrea P, Messina C, Reggio A, Bresciamorra V, Orefice G, Paciello M, Brunetti A, Coniglio G, Bonavita S, Di Costanzo A, Bellacosa A, Valentino P, Quarantelli M, Patti F, Salemi G, Cammarata E, Simone IL, Salvatore M, Bonavita V, Alfano B. Brain atrophy and lesion load in a large population of patients with multiple sclerosis. Neurology 2005;65:280-285.

Truyen L, van Waesberghe JH, van Walderveen MA, van Oosten BW, Polman CH, Hommes OR, Adèr HJ, Barkhof F. Accumulation of hypointense lesions ("black holes") on T1 spin-echo MRI correlates with disease progression in multiple sclerosis. Neurology 1996;47:1469-1476.

Tung GA, Rogg JM. Diffusion-weighted imaging of cerebritis. AJNR Am J Neuroradiol 2003;24:1110-1113.

Turner R, Le Bihan D, Maier J, Vavrek R, Hedges LK, Pekar J. Echo-planar imaging of intravoxel incoherent motion. Radiology 1990;177:407-414.

Ulrich K, Tröscher-Weber R, Tomandl BF, Neundörfer B, Reinhardt F. Posterior reversible encephalopathy in eclampsia: diffusion-weighted imaging and apparent diffusion coefficient-mapping as prognostic tools? Eur J Neurol 2006;13:309-310.

Vaneckova M, Kalincik T, Krasensky J, Horakova D, Havrdova E, Hrebikova T, Seidl Z. Corpus callosum atrophy--a simple predictor of multiple sclerosis progression: a longitudinal 9-year study. Eur Neurol 2012;68:23-27.

van Walderveen MA, Kamphorst W, Scheltens P, van Waesberghe JH, Ravid R, Valk J, Polman CH, Barkhof F. Histopathologic correlate of hypointense lesions on T1-weighted spin-echo MRI in multiple sclerosis. Neurology 1998;50:1282-1288.

van Walderveen MA, Tas MW, Barkhof F, Polman CH, Frequin S, Hommes OR, Valk J. Magnetic resonance evaluation of disease activity during pregnancy in multiple sclerosis. Neurology 1994;44:327-329.

Virtanen SM, Lindroos MM, Majamaa K, Nuutila P, Borra RJ, Parkkola R. Voxelwise analysis of diffusion tensor imaging and structural MR imaging in patients with the m.3243A>G mutation in mitochondrial DNA. AJNR Am J Neuroradiol 2011;32:522-526.

Vollmer T, Ni W, Stanton S, Hadjimichael O. The NARCOMS patient registry: a resource for investigators., Int J MS Care, 1999;1:12-15.

Vrenken H, Geurts JJ, Knol DL, Polman CH, Castelijns JA, Pouwels PJ, Barkhof F. Normal-appearing white matter changes vary with distance to lesions in multiple sclerosis. AJNR Am J Neuroradiol 2006;27:2005-2011.

Vukusic S, Confavreux C. Pregnancy and multiple sclerosis: the children of PRIMS. Clinical Neurol Neurosurg 2006;108:266-270.

Vukusic S, Hutchinson M, Hours M, Moreau T, Cortinovis-Tourniaire P, Adeleine P, Confavreux C, the Pregnancy In Multiple Sclerosis Group. Pregnancy and multiple sclerosis (the PRIMS study): clinical predictors of post-partum relapse. Brain 2004;127:1353-1360.

Watanabe Y, Mitomo M, Tokuda Y, Yoshida K, Choi S, Hosoki T, Ban C. Eclamptic encephalopathy: MRI, including diffusion-weighted images. Neuroradiology 2002;44:981-985.

Watson R, Blamire AM, Colloby SJ, Wood JS, Barber R, He JB, O'Brien JT. Characterizing dementia with Lewy bodies by means of diffusion tensor imaging. Neurology 2012;79:906-914.

Werring DJ, Brassat D, Droogan AG, Clark CA, Symms MR, Barker GJ, MacManus DG, Thompson AJ, Miller DH. The pathogenesis of lesions and normal-appearing white matter changes in multiple sclerosis: a serial diffusion MRI study. Brain 2000;123:1667-1676.

Wheeler-Kingshott CA, Cercignani M. About "axial" and "radial" diffusivities. Magn Reson Med 2009;61:1255-1260.

Whybra C, Miebach E, Mengel E, Gal A, Baron K, Beck M, Kampmann C. A 4-year study of the efficacy and tolerability of enzyme replacement therapy with agalsidase alfa in 36 women with Fabry disease. Genet Med 2009;11:441-449.

Wiendl H, Toyka KV, Rieckmann P, Gold R, Hartung HP, Hohlfeld R; Multiple Sclerosis Therapy Consensus Group (MSTCG). Basic and escalating immunomodulatory treatments in multiple sclerosis: current therapeutic recommendations. J Neurol 2008;255:1449-1463.

Wilcox WR, Oliveira JP, Hopkin RJ, Ortiz A, Banikazemi M, Feldt-Rasmussen U, Sims K, Waldek S, Pastores GM, Lee P, Eng CM, Marodi L, Stanford KE, Breunig F, Wanner C, Warnock DG, Lemay RM, Germain DP. Females with Fabry disease frequently have major organ involvement: Lessons from the fabry registry. Mol Genet Metab 2008;93:112-128.

Wu CM, Ng SH, Liu TC. Diffusion tensor imaging of the subcortical auditory tract in subjects with long-term unilateral sensorineural hearing loss. Audiol Neurootol 2009;14:248-253.

Yong VW, Chabot S, Stuve O, Williams G. Interferon beta in the treatment of multiple sclerosis: mechanisms of action. Neurology 1998;51:682-689.

Yong VW. Differential mechanisms of action of interferon-beta and glatiramer acetate in MS. Neurology 2002;59:802-808.

Zarate YA, Hopkin RJ. Fabry's disease. Lancet 2008;372:1427-1435.

Zeeman GG, Hatab M, Twickler DM. Maternal cerebral blood flow changes in pregnancy. Am J Obstet Gynecol 2003;189:968-972.

Zhang YY, Brady M, Smith S. Segmentation of brain MR images through a hidden Markov random field model and the expectation-maximization algorithm. IEEE Trans Med Imaging 2001;20:45-57.